Chapter 12: Multiscale Modeling for Damage Analysis

Ramesh Talreja and Chandra Veer Singh

Department of Aerospace Engineering, Texas A&M University,
College Station, TX 77843-3141, USA

12.1 Introduction

The increased computational power and programming capabilities in recent years have given impetus to the so-called *multiscale modeling*, which implements the largely intuitive notion that physical phenomena occurring at a lower length or size scale determine the observed response at a higher scale. A logical outcome of this thought is an organization of differentiated scales – from the lowest, such as nanometer scale, to the highest scale typical of the part or structure in mind – giving a hierarchy of scales. Working up the scales produces a hierarchical multiscale modeling, in which the essential challenge consists of "bridging" the scales. The simulation techniques, such as molecular dynamics simulation (MDS), succeed mostly in revealing phenomena from one scale to the next; but proceeding to three or more scales often necessitates unrealistic computing power even with the most versatile facilities available. In addition, the limitation of independent physical validation of the simulated results questions the wisdom of total reliance on the multiscale hierarchical modeling strategy.

When it comes to subcritical (prefailure) damage in composites, the multiscale modeling concept needs closer examination, firstly, because the length scales of constituents and heterogeneities are fixed while those of damage evolve progressively, and secondly, because the mechanisms of damage tend to segregate in modes with individual characteristic scales. All this is the subject of this chapter, which will first describe and clarify the damage mechanisms in common types of composites followed by the induced response observed at the macroscale. The hierarchical modeling

approach will be discussed against this knowledge; and a different approach, named *synergistic multiscale modeling*, will be advocated. Assessment will be offered of the current state of this modeling, and future activities aimed at accomplishing its objectives will be outlined.

The following treatment of multiscale modeling will draw upon a recent paper by Talreja [61] as well as other previous works.

12.2 Phenomenon of Damage in Composite Materials

Engineered structures must be capable of performing their functions throughout a specified lifetime while being exposed to a series of events that include loading, environment, and damage threats. These events, either individually or in combination, can cause structural degradation, which, in turn, can affect the ability of the structure to perform its function. The performance degradation in structures made of composites is quite different when compared to metallic components because the failure is not uniquely defined in composite materials. To understand how composites may lose the ability to perform satisfactorily, some basic definitions related to damage of composite materials must be reviewed. Section 12.2.1 contains a brief overview of significant mechanisms that can degrade a composite material.

In a conventional sense, *fracture* is understood to be "breakage" of material, or at a more fundamental level, breakage of atomic bonds, which manifests itself in formation of internal surfaces. Examples of fractures in composites are fiber fragmentation, cracks in matrix, fiber/matrix debonding, and separation of bonded plies (delamination). The field of fracture mechanics concerns itself with conditions for enlargement of the surfaces of material separation.

Damage refers to a collection of all the irreversible changes brought about by energy dissipating mechanisms, of which atomic bond breakage is an example. Unless specified differently, damage is understood to refer to distributed changes. Examples of damage are multiple fiber-bridged matrix cracking in a unidirectional composite, multiple intralaminar cracking in a laminate, local delamination distributed in an interlaminar plane, and fiber/matrix interfacial slip associated with multiple matrix cracking. These damage mechanisms are explained in some detail in Sect. 12.2.1. The field of damage mechanics deals with conditions for initiation and progression of distributed changes as well as consequences of those changes on the response of a material (and by implication, a structure) to external loading.

Failure is defined as the inability of a given material system (and consequently, a structure made from it) to perform its design function. Fracture

is one example of a possible failure; but, generally, a material could fracture (locally) and still perform its design function. Upon suffering damage, e.g., in the form of multiple cracking, a composite material may still continue to carry loads and, thereby, meet its load-bearing requirement but fail to deform in a manner needed for its other design requirements, such as vibration characteristics and deflection limits.

Structural integrity is defined as the ability of a load-bearing structure to remain intact or functional upon the application of loads. In contrast to metals, remaining intact (not breaking up in pieces) for composites is not necessarily the same as remaining functional. Composites can lose their functionality by suffering degradation in their stiffness properties while still carrying significant loads.

12.2.1 Mechanisms of Damage

Due to extreme levels of anisotropy and inhomogeneity of composites, a variety of damage mechanisms cause degradation in the material behavior. These can occur separately or in combination. A short description of each damage mechanism follows.

Multiple matrix cracking

Matrix cracks are usually the first observed form of damage in composite laminates [45]. These are intralaminar or ply cracks, transverse to loading direction, traversing the thickness of the ply and running parallel to the fibers in that ply. The terms *matrix microcracks*, *transverse cracks*, *intralaminar cracks*, and *ply cracks* are invariably used to refer to this very same phenomenon. Matrix cracks are observed during tensile loading, fatigue loading, changes in temperature, and thermocycling. Figure 12.1

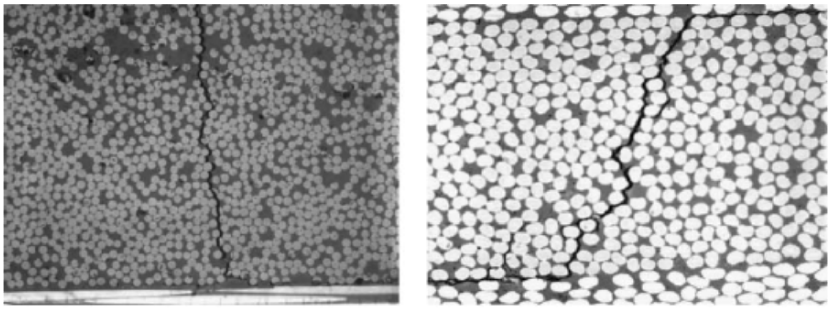

Fig. 12.1. Examples of matrix cracks observed on the free edges induced due to fatigue loading in composite laminates [37]

illustrates matrix cracks observed on the free edges induced due to fatigue loading in composite laminates [37]. Although matrix cracking does not cause structural failure by itself, it can result in significant degradation in material stiffness and also can induce more severe forms of damage, such as delamination and fiber breakage [44]. Numerous studies of microcracking initiation were performed in the 1970s and early 1980s [4, 13–15, 29, 48, 49]. It was observed that the strain to initiate microcracking increases as the thickness of 90° plies decreases. Also, these microcracks form almost instantaneously across the width of the specimen.

The first attempt to predict the strain to first microcrack used the *first ply failure* theory [18] where it is assumed that the first crack develops when the strain in the plies reaches the strain to failure in the plies. The predictions were not in agreement with the experimental observations since the first ply failure theory predicts that the strain to initiate microcracking will be independent of the ply thickness. The experimental observations on laminates with a 90° layer on the surface $[90_n/0_m]_s$ show that the strain to initiate microcracking is lower for laminates with cracks in surface plies than for laminates with cracks in central plies [52, 54].

The simplest way to model transverse matrix cracks in composite laminates is to completely neglect the transverse stiffness of cracked plies, called the *ply discount method*. This method underestimates the stiffness of cracked laminates, since cracked plies, in reality, can take some loading. Another simple way is *shear lag analysis*, wherein the load transfer between plies is assumed to take place in shear layers between neighboring plies. The normal stress in the external load direction is assumed to be constant over the ply thickness. The thicknesses and stiffness of these shear layers are generally unknown, and the variations in the thickness direction of local ply stresses and strains are also neglected in the shear lag theory. The shear lag theory has limited success for crossply laminates [19, 25, 39, 62]. For crossply laminates, the most successful approach is the *variational method*. By application of the principle of minimum complementary potential energy, Hashin [21, 22] derived estimates for thermomechanical properties and local ply stresses, which were in good agreement with experimental data. Varna and Berglund [65] later made improvements to the Hashin model by use of more accurate trial stress functions. A disadvantage of the variational method is that it is extremely difficult to use for laminate layups other than crossplies. McCartney [43] used Reissner's energy function to derive governing equations similar to Hashin's model. He applied this approach to doubly cracked crossply laminates assuming that the in-plane normal stress dependence on the two in-plane coordinates is given by two independent functions. Gudmundson and coworkers [16, 17] considered

laminates with general layup and used the homogenization technique to derive expressions for stiffness and thermal expansion coefficient of laminates with cracks in layers of three-dimensional (3D) laminates. These expressions correlate damaged laminate thermoelastic properties with parameters characterizing crack behavior: the average crack opening displacement (COD) and the average crack face sliding. These parameters follow from the solution of the local boundary value problem, and their determination is a very complex task. Also, the effect of neighboring layers on crack face displacements was neglected; and the displacements were determined assuming a periodic system of cracks in an infinite homogeneous, transversely isotropic medium (90° layer). The application of their methodology by other researchers has been rather limited due to the fairly complex form of the presented solutions.

An alternative way to describe the mechanical behavior of matrix-cracked laminates is to apply concepts of damage mechanics. Generally speaking, the continuum damage mechanics (CDM) approaches [1, 2, 56, 57] may be used to describe the stiffness of laminates with intralaminar cracks in off-axis plies of any orientation. The damage is represented by internal state variables (ISVs), and the laminate constitutive equations are expressed in general forms containing ISV and a certain number of material constants. These constants must be determined for each laminate configuration considered either experimentally, measuring stiffness for a laminate with a certain crack density, or using finite element (FE) analysis. This limitation is partially removed in synergistic damage mechanics (SDM) suggested by Talreja [60], which incorporates micromechanics information in determining the material constants. The SDM approach has proved to be quite efficient for a variety of laminate layups and material systems. The present chapter builds on this methodology, and relevant details will be discussed later.

Interfacial debonding

The performance of a composite is markedly influenced by the properties of the interface between the fiber and matrix resin. The adhesion bond at the interfacial surface affects the macroscopic mechanical properties of the composite. The interface plays a significant role in stress transfer between fiber and matrix. Controlling interfacial properties thus leads to the control of composite performance. In unidirectional composites, debonding occurs at the interface between fiber and matrix when the interface is weak. The longitudinal interfacial debonding behavior of single-fiber composites has been studied in detail by the use of the pullout [26, 38, 73] and fragmentation [10, 12, 24, 72] tests. The mechanics of interfacial debonding in

a unidirectional fiber-reinforced composite are depicted in Fig. 12.2. When fracture strain of the fiber is greater than that of the matrix, i.e., $\varepsilon_f > \varepsilon_m$, a crack originating at a point of stress concentration, e.g., voids, air bubbles, or inclusions, in the matrix is either halted by the fiber, if the stress is not high enough, or it may pass around the fiber without destroying the interfacial bond (Fig. 12.2a). As the applied load increases, the fiber and matrix deform differentially, resulting in a buildup of large local stresses in the fiber. This causes local Poisson contraction; and eventually shear force developed at the interface exceeds the interfacial shear strength, resulting in interfacial debonding at the crack plane that extends some distance along the fiber at the interface (Fig. 12.2c).

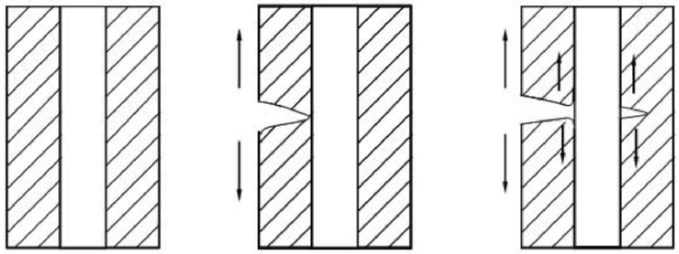

Fig. 12.2. Mechanics of interfacial debonding in a simple composite [20]

Interfacial sliding

Interfacial sliding between constituents in a composite can take place by differential displacement of the constituents. One example of this is when fibers and matrix in a composite are not bonded together adhesively but by a "shrink-fit" mechanism, due to difference in thermal expansion properties of the constituents. On thermomechanical loading, the shrink-fit (residual) stresses can be removed, leading to a relative displacement (sliding) at the interface. The relief of interfacial normal stress can also occur when a matrix crack tip approaches or hits the interface.

When the two constituents are bonded together adhesively, interfacial sliding can occur subsequent to debonding if a compressive normal stress on the interface is present. The debonding can be induced by a matrix crack, or it can result from growth of interfacial defects. Thus, interfacial sliding that follows debonding can be a separate damage mode or it can be a damage mode coupled with matrix damage.

When the interface between the matrix and the fiber debonds, this relieves the tensile residual stresses in the matrix. Due to different stresses in the matrix and the fiber at the interface, the fibers slide on the interfacial surface. Subsequently, the sliding surfaces cause degradation of material due to frictional wear at the interface. Pullout and pushback tests are useful in determining the stress required to cause interfacial sliding. This mostly depends upon the strength of the adhesive bond between the matrix and the fiber at the interface.

Fiber microbuckling

When a unidirectional composite is loaded in compression, the failure is governed by the matrix and occurs through a mechanism known as *microbuckling of fibers*. There are two basic modes of microbuckling deformation: "extensional" and "shear" modes [51], as shown in Fig. 12.3, depending upon whether the fibers deform "out of phase" or "in phase." The compressive strength corresponds to the onset of instability and is given as

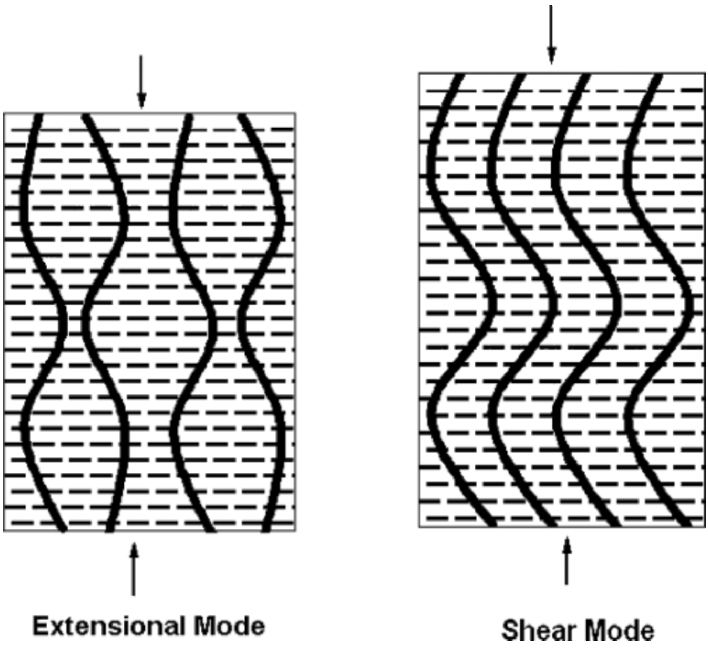

Fig. 12.3. Extensional and shear modes of microbuckling [51]

$$\sigma_c = 2V_f \sqrt{\frac{V_f E_f E_m}{3(1-V_f)}} \tag{12.1}$$

for the extension mode and

$$\sigma_c = \frac{G_m}{1-V_f} \tag{12.2}$$

for the shear mode, where E and G denote Young's modulus and shear modulus, respectively, and subscripts "f" and "m" designate fiber and matrix, respectively.

Although these expressions are based on energy balance, they do not agree with experimental observations. As an alternative, it has been argued that manufacturing of composites tends to cause misalignment of fibers, which can induce localized kinking of fiber bundles. The kinking process is driven by local shear, which depends on the initial misalignment angle ϕ_0 [3]. The critical compressive stress corresponding to instability is given by

$$\sigma_c = \frac{\tau_y}{\phi_0}, \tag{12.3}$$

where τ_y represents the interlaminar shear strength. Budiansky [6] considered the kink band geometry and derived the following estimate for the kink band angle β in terms of the transverse modulus E_T and shear modulus G of a two-dimensional (2D) composite layer:

$$(\sqrt{2}-1)^2 \frac{G-\sigma_c}{E_T} < \tan^2 \beta < \frac{G-\sigma_c}{E_T}. \tag{12.4}$$

To account for shear deformation effects, Niu and Talreja [46] modeled the fiber as a generalized Timoshenko beam with the matrix as an elastic foundation. It was observed that not only an initial fiber misalignment but also any misalignment in the loading system can affect the critical stress for kinking.

Delamination

Delamination as a result of low-velocity impact loading is a major cause of failure in fiber-reinforced composites [7, 9, 40]. Delamination can occur below the surface of a composite structure with a relatively light impact, such as that from a dropped tool, while the surface remains undamaged to visual inspection [9, 28, 50]. The growth of delamination cracks under the subsequent application of external loads leads to a rapid deterioration of the mechanical properties and may cause catastrophic failure of the com-

posite structure [55]. Delamination is a substantial problem because the composite laminates, although having strength in the fiber direction, lack strength in the through-thickness direction. This essentially limits the strength of a traditional 2D composite to the properties of the brittle matrix alone [71]. The development of interlaminar stresses is the primary cause of delamination in laminated fibrous composites. Delamination occurs when the interlaminar stress level exceeds the interlaminar strength. The interlaminar stress level is associated with the specimen geometry and loading parameters, while the interlaminar strength is related to the material properties [40, 71]. From an energy point of view, delamination cracks will grow when the energy required to overcome the cohesive force of the atoms is equal to the dissipation of the strain energy that is released by the crack [11]. The delamination can be reduced by either improving the fracture toughness of the material or modifying the fiber architecture [8, 42].

Typically, a low-speed impact overstresses the matrix material, producing local subcritical cracking (microcracking). This does not necessarily produce fracture; however, it will result in stress redistribution and the concentration of energy and stress at the interply regions where large differences in material stiffness exist. The onset and rapid propagation of a crack results in sudden variations in both section properties and load paths within the composite local to the impactor. This requires an adaptive method to track the progression of damage and fracture growth.

Fiber fracture

As the applied load is increased, progressive matrix cracks lead to fiber/matrix interfacial debonding and delamination; and the stress state inside laminate material becomes quite complex. Ultimately, when the laminate strain reaches fiber failure strain, the fibers start to fail; and multiple cracks develop in the fibers. The multiple fiber cracks also develop due to stress transfer in the regions where the matrix is not able to take any more load.

Since at this load level other damage modes are also present, the real reason for ultimate failure is often not clear. At ultimate failure load, the matrix is shattered; and, evidently, the fibers carry the full failure load. The composites usually support large load and deformation at failure, although the measured ultimate strength clearly may not be reliable in actual applications [47]. All fibers are not of the same strength, and a statistical variation of strength between fibers and along fiber lengths is used. In addition to strength and modulus, another important property of a fiber-reinforced composite is its resistance to fracture. The fracture toughness of a composite depends not only on the properties of the constituents but also significantly on the efficiency of bonding across the interface [33].

The damage mechanisms described above have different characteristics depending on a variety of geometric and material parameters. Each mechanism has different governing length scales and evolves differently when the applied load is increased. Interactions between individual mechanisms further complicate the damage picture. As the loading increases, stress transfer takes place from a region of high damage to that of low damage, and the composite failure results from the criticality of the last load-bearing element or region. For clarity of treatment, the full range of damage can be separated into damage modes, treating them individually followed by examining their interactions. This approach will be discussed in detail in later sections with respect to ceramic matrix composites (CMCs) and polymer matrix composites (PMCs).

12.2.2 Damage-Induced Response of Composites

The presence of damage in a composite induces *permanent* changes in the response with respect to the virgin state. One objective of multiscale modeling is to relate these changes to the damage, specifically taking into account the scale(s) at which damage mechanisms operate. In this section, a simple case of unidirectional continuous fiber composites, which respond linear elastically in the virgin state, will be examined to illustrate how the response can be varied when multiple matrix cracking damage exists. Two cases will be considered (1) a constrained PMC loaded in tension transverse to fibers and (2) an unconstrained CMC loaded in tension along fibers.

Constrained PMC loaded in tension transverse to fibers

When a unidirectional PMC is loaded in uniform tension normal to fibers, it responds linear elastically until failure initiates from matrix or interfacial cracking. However, if this composite is bonded to stiff elastic elements and then loaded, still transverse to fibers, its failure changes from single fracture to multiple matrix cracking as described above. The response of the combined composite and the stiff elements changes as the multiple cracking progresses, i.e., its intensity, measured by, e.g., crack number density, increases. The changes in response induced by cracking depend on the constraining effect of the stiff elements. This phenomenon is conveniently illustrated in Fig. 12.4 by an axially loaded crossply composite $[0_m/90_n]_s$ in which the degree of constraint to transverse ply cracking can be varied by selecting the m/n ratio. Considering the strain ε_{FPF} at which first cracking occurs in the constrained transverse ply, Talreja [56] classified the constraint in four categories (Fig. 12.5) (A) no constraint, (B)

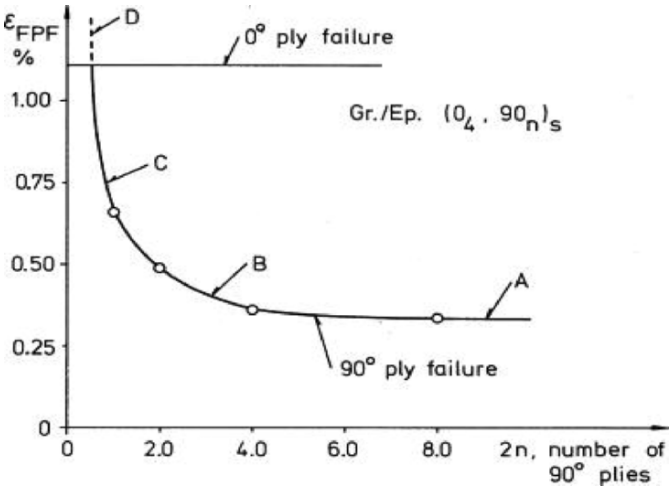

Fig. 12.4. The strain at first ply failure as a function of the number of transverse plies in $[0_4/90_n]_s$ laminate

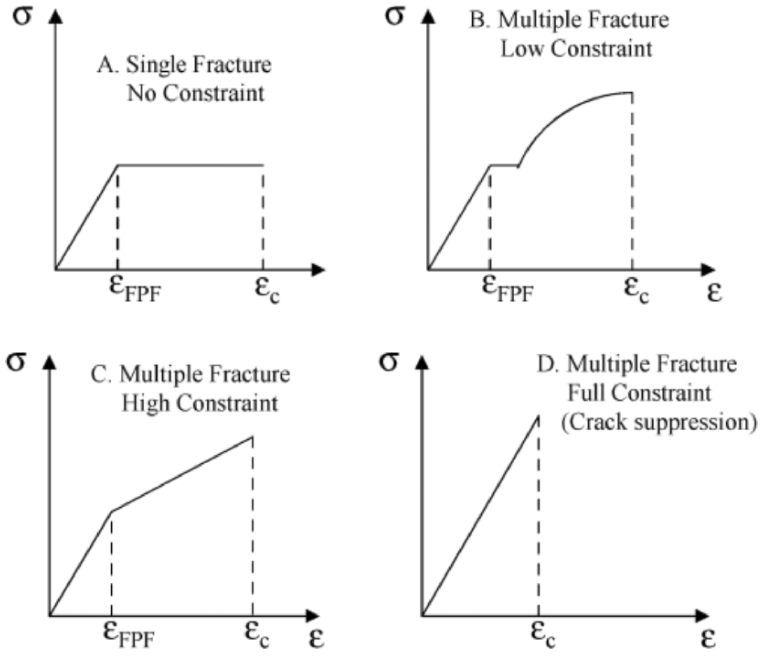

Fig. 12.5. Stress–strain response at different constraints to transverse cracking in crossply laminates

low constraint, (C) high constraint, and (D) full constraint. In the case of $[0_4/90_n]_s$ laminate, ε_{FPF} varies with the number $2n$ of 90° plies. As this number increases, the constraint of the 0° plies becomes increasingly insignificant and ε_{FPF} approaches the failure strain of the unconstrained 90° plies, i.e., the failure strain normal to fibers. On the other extreme, as the constraint of the 0° plies becomes effective, this strain increases; and multiple cracking occurs. This process continues to higher constraint; and at some point, the ε_{FPF} exceeds the fiber failure strain, at which point the constraining plies fail.

Unconstrained CMC loaded in tension along fibers

The stress–strain response of a unidirectional CMC loaded in axial tension is described in Fig. 12.6. This response develops in stages as the matrix cracking progresses, as evidenced by the set of micrographs obtained by Sørensen and Talreja [53] shown in Fig. 12.7. The micrograph taken at 0.15% axial strain shows the matrix cracks normal to the (horizontal) fiber axis that do not span the complete specimen cross section. As strain increases, more cracks form and quickly span the whole specimen width. Finally, the cracking saturates, i.e., no more cracks form on increasing the load. This stage of progressive matrix cracking represents Stage II, extending from 0.13 to 0.5% axial strain in Fig. 12.6. The preceding stage (Stage I) consists of linear elastic behavior before the onset of cracking. Beyond 0.5%

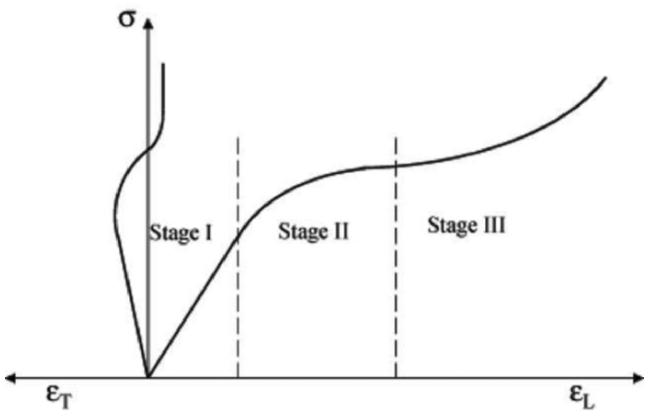

Fig. 12.6. The three stages of stress–strain response in a SiC fiber-reinforced glass-ceramic composite [53]

strain, the frictional sliding at the fiber/matrix interface becomes significant. Finally, beyond 0.7% strain, a progressive fiber breakage takes place leading to localization of damage and catastrophic failure. The Stage II progressive cracking was treated by Sørensen and Talreja [53]. In Sect. 12.3, two cases of damage will be used to illustrate the multiscale nature of damage and discuss how the scales can be incorporated into a damage mechanics framework.

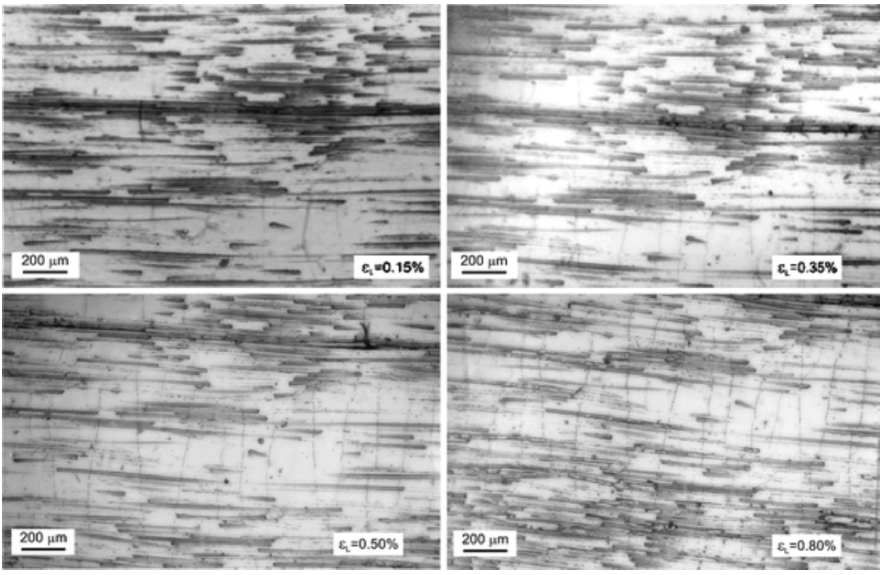

Fig. 12.7. Surface micrographs of a SiC fiber-reinforced glass-ceramic composite at different axial strains. Tensile loading was in the (*horizontal*) fiber direction [53]

12.3 Multiscale Nature of Damage

As described in Sect. 12.2, the damage in composites occurs due to a variety of dissipative mechanisms which cause permanent changes in the internal microstructure of the material and decrease the energy storing capacity of the material. The most basic scale at which these mechanisms occur depends upon the size of inhomogeneities in the microstructure of the material. As an example, nanocomposites may show dissipative mechanisms at the nanometer scale. In reality, however, identifying this scale is limited by the ability to observe as well as to model and analyze the

mechanisms at the observed scale. The so-called microscale is a reference to the scale at which entities or features within a material are observable by a certain type of microscope. Thus, for example, the microscale can be a few micrometers, if an electron microscope is used to observe entities, such as cracks or crystalline slip within grains or at grain boundaries. The scale reduces by an order of magnitude if one focuses on dislocations observed by a transmission electron microscope. Today, the use of nano-scale elements (particles, fibers, tubes, etc.) has moved the basic scale further down to the atomic scale. At this scale, the basic notions of continuum mechanics fail; and it is necessary to develop modeling tools that can bridge the discrete-level descriptions (quantum mechanics) to continuum-type (smeared-out) descriptions.

In an engineering approach, the purpose at hand should guide the choice of the basic scale. Thus, if the overall (effective) characteristics of inelastic response are of interest, it would suffice to incorporate the energy dissipating mechanisms in a model, directly or indirectly, in an appropriate average sense; while if, for instance, the aim is a particular material failure characteristic, the analysis may need to be conducted at the local physical scale of the relevant details of the mechanisms. On the other hand, if the purpose is to design a material, i.e., to engineer its response or to provide it with certain functionalities, then it would be necessary to address scales where the material (micro) structure can be modified, manipulated, or intruded.

In composite materials, the scales of inhomogeneities (reinforcements, additives, second phases, etc.) embedded in the baseline material (matrix) determine the characteristic scales of operation of the mechanisms of energy dissipation. Although energy dissipation may also be occurring at other (smaller) scales, e.g., the scale of the matrix material's microstructure, the dissipative mechanisms associated with the inhomogeneities have usually an overriding influence on the composite behavior. For instance, in short-fiber PMCs, the size of fiber diameter manifests the scale at which matrix cracks form, although energy dissipation may also occur at the matrix polymer's molecular scale.

The complexity introduced by inhomogeneities in composite damage is in the form of multiple scales of dissipative mechanisms depending on the geometrical features of the inhomogeneities. In the case of short fibers, for instance, the matrix cracking from the fiber ends and the fiber/matrix debonding occurs at two length scales, determined by the fiber diameter and fiber length, respectively. For composite laminates, the thickness of identically oriented plies sets the scale for development of intralaminar cracking, while for formation of these cracks the appropriate scale is given by the fiber diameter. Thus, in modeling of a composite material's behavior,

one faces a complex situation concerning the length scales; and taking a hierarchical approach may not be efficient, as will be discussed later. In the following, the multiscale nature of damage in composite materials will be illustrated by examining the two cases pertaining to damage in unidirectional CMCs and ply cracking in laminates.

12.3.1 Unidirectional CMCs

In the case of CMCs, the fiber/matrix interfacial region has a strong influence on the thermomechanical response. The properties of the interfacial region determine whether a matrix crack front approaching a fiber advances into the fiber or bypasses it by causing interfacial slip and/or debonding. The damage configurations at the microscopic level thus generated govern the macroscopic (overall) response of a composite. There are three basic mechanisms of damage in CMCs: matrix cracking, interfacial sliding, and interfacial debonding. They can occur independently or interactively. The experimental evidence indicates that the interfacial damage (slip and debonding) occurs primarily in conjunction with matrix cracking [41]. Talreja [59] used these damage configurations to characterize damage, as shown in Fig. 12.8a–d. Figure 12.8b,d shows interfacial slip and debonding, both in conjunction with matrix cracking. This situation (b) will result if the fibers are held in the matrix by frictional forces at the interfaces, while (d) is likely to result from a nonuniform interfacial bond strength [59].

The characterization of damage is done by regarding damage entities as internal structure of the homogeneous body. The internal structure changes with loading and causes changes of the overall response of the composite. The internal structure of a continuum is described using the so-called *internal variables*. These variables are some appropriately defined quantities representing the geometry, i.e., size, shape, orientation, etc., of the internal structure as well as the influence of the internal structure on the response considered. The quantities chosen depend on the geometrical characteristics of the entities involved in the internal structure constitution and the nature of the influence of these entities on the response of the composite. The elementary damage entities present in the damage configurations treated here are cracks, debonds, and slipped surfaces. The characterization used for cracks and debonds is different from that used for slipped surfaces. These two types are, therefore, treated separately in the following.

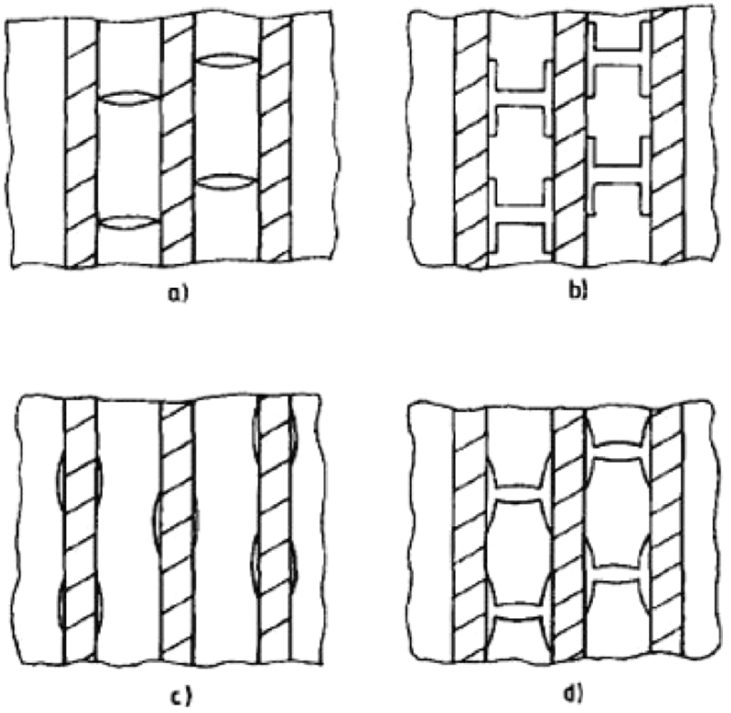

Fig. 12.8. Distributed damage configurations in CMCs: (**a**) matrix cracking, (**b**) interfacial slip in conjunction with matrix cracking, (**c**) debonding, and (**d**) debonding in conjunction with matrix cracking [59]

Matrix cracking

A matrix crack can be viewed as a pair of internal surfaces in a composite that are able to perturb the stress state in a region around the surfaces by conducting displacement, i.e., separation of surfaces, from the undeformed configuration. The surface separation per unit of applied external load depends on the size and shape of the surfaces as well as on the constraint, if any, imposed by the surroundings. For a matrix crack in a unidirectional CMC, the constraint comes from the bridging fibers as well as from the stiffening effect of fibers in the matrix surrounding the crack.

The description for matrix cracks follows a second-order tensor characterization as suggested first by Vakulenko and Kachanov [64] and described in further detail by Kachanov [31]. Talreja [58] used a diad an to characterize a damage entity of a finite volume bounded by a surface S. In this characterization, n is the unit outward normal to the surface at a point

on the surface and a represents the extent and direction of some "influence," e.g., the disturbance of the strain fields, due to presence of the damage entity, referred to the same point on the surface. A "damage entity tensor" is then defined as

$$d_{ij} = \int_S a_i n_j \mathrm{d}S, \tag{12.5}$$

with reference to a Cartesian coordinate system X_i. The influence vector can be resolved along the normal and tangential directions with respect to the crack surface. For the type of crack considered here, it is reasonable to assume that only the normal (crack opening) displacement matters, allowing a_i to be expressed as

$$a_i = an_i, \tag{12.6}$$

where the quantity a now represents a measure of the crack influence. From dimensional analysis, with d_{ij} taken to be dimensionless, a has dimensions of length. Drawing upon fracture mechanics, this length is in proportion to the crack length. For a fiber-bridged matrix crack, the crack length l can be expressed in multiples of the average interfiber spacing. Thus,

$$l = kd\frac{1-\sqrt{v_\mathrm{f}}}{\sqrt{v_\mathrm{f}}}, \tag{12.7}$$

where k is a constant, d is the fiber diameter, and v_f is the fiber volume fraction. The expression in (12.7) is based on a hexagonal fiber arrangement. Similar expression will result from another assumption of fiber distribution in the cross section. It can now be inferred that the microstructural *length scale* for matrix microcracking is the fiber diameter. Note that, for an irregularly shaped crack surface, the interfiber spacing and, therefore, the fiber diameter will still be the length scale.

The consequence of the presence of a matrix crack is generally in changing the composite's deformational response, which is defined and measured at a larger length scale, e.g., the characteristic length of a volume containing a representative sample of the cracks. This volume is called a *representative volume element* (RVE). For the Stage II stress–strain response [53], the model proposed in [59] was used. Accordingly, assuming the influence vector magnitude a to be proportional to the crack length,

$$a = \kappa l, \tag{12.8}$$

where l is a constant representing the constraint to the crack surface displacement. This constant equals zero when the constraint allows no crack separation, while it increases as the constraint reduces. From (12.5), (12.6), and (12.8), the damage entity tensor for matrix cracking is

$$d_{ij}^{\mathrm{mc}} = \kappa l^2 t n_i n_j, \tag{12.9}$$

where t is the specimen thickness (or the through-thickness characteristic dimension of the crack).

The macrolevel deformational response is derived from a strain energy density function that depends on the strain and damage states. The matrix-cracking damage state is characterized by Talreja [59]

$$D_{ij}^{\mathrm{mc}} = \frac{1}{V}\sum d_{ij}^{\mathrm{mc}}, \tag{12.10}$$

where V is the RVE volume of an RVE over which the summation is conducted. Substituting (12.5) in (12.6), one obtains

$$D^{\mathrm{mc}} = \kappa \eta A \langle fl \rangle, \tag{12.11}$$

where $D^{\mathrm{mc}} = D_{11}^{\mathrm{mc}}$ is the only surviving component of the damage mode tensor, f is the fraction of RVE width spanned by a crack, η is the crack number density, i.e., the number of cracks per unit volume, and A is the cross-sectional area. The quantity within the brackets $\langle\,\rangle$ is averaged over the RVE volume.

The matrix crack length (12.7) appears in the damage descriptor (12.11). As shown in [59], the crack length also governs the elastic constants at a given crack density η. For instance, the axial Young's modulus can be written as

$$E_{11} = E_{11}^0 (1 - c\eta l), \tag{12.12}$$

where c is a constant and the superscript 0 is for the initial value.

In characterizing matrix cracks as a damage mode, no specific account is made of the associated fiber/matrix debonding and sliding mechanisms. These can be considered separately and then accounted for by their interactions with the matrix cracks [59]. Discussions of these mechanisms follow.

Interfacial debonding

The fiber/matrix interface can debond due to several causes. Essentially, a stress normal to fibers or a shear stress along fibers, or a combination of the two, must exist for the bond to fail. These stresses can be generated by

a fiber break or brought into play by an approaching matrix crack. Alternatively, a preexisting flaw at the fiber surface or an imperfect fiber, or its misalignment, can produce those stresses. If debonds are produced without interaction with matrix cracks, then they can be characterized in a manner similar to matrix cracks. A characterization of such distributed debonding is given in [59] based on certain simplifying assumptions. The only surviving damage mode tensor component for this case is D_{22}, and its form is the same as that of D_{mc} in (12.11). Thus, the debond length and the debond number density enter into the damage mode description. The debond length will depend on the characteristic flaw length, which in turn depends on the manufacturing process. Unless the ability of the manufacturing process to produce interfacial flaws somehow depends on the composite microstructure, no microstructural length scale can be identified for the debonding mechanism.

In the case of a matrix crack initiating debonding and then merging with the debond crack, more force on the advancing debond crack comes from the opening displacement of the matrix crack. The damage configuration of interest, then, is not the debond crack itself but a combined matrix-debond crack. The latter can be viewed as a fiber-bridged matrix crack, discussed above, with the constraint to its surface displacement now modified by the presence of debonding. Then, the constant α in (12.8), (12.9), and (12.11) may be changed to another value, resulting in a change of the constant c in (12.12).

Thus, for debonding that occurs in conjunction with matrix cracking, the determining length associated with the damage mode is still the matrix crack length l, although with a modified influence. This length can still be expressed by (12.7), giving the fiber diameter as the microstructural length scale.

Specific treatments of debonding by itself and debonding in conjunction with matrix cracking are given in [59]. Based on that work, the axial modulus for the latter case can be modified from (12.12) to be

$$E_{11} = E_{11}^0(1 - c'\eta l), \tag{12.13}$$

Where

$$c' = c + k_1 d_1, \tag{12.14}$$

where d_1 is the ratio of the debond length to the crack length and k_1 is a constant. Here, a fixed ratio of the number of debonds per unit of matrix crack length has been assumed.

From (12.13) and (12.14), it can be seen that the debond length does not enter into the RVE response directly but via its ratio to the crack length, suggesting that the governing length for this response is the crack length.

Interfacial sliding

Interfacial sliding occurs when fibers and matrix remain in contact after debonding of the interface and undergo unequal displacements. Talreja [59] defined a measure of the slip at the interface as the area swept off by the relative displacement of one constituent over the other and expressed this measure in terms of a slippage vector. A slippage tensor was then constructed as a dyadic product of the slippage vector with itself to account for the insensitivity of the material response to the direction of slip. As in the case of debonding, discussed previously, when sliding occurs in conjunction with matrix cracking, the slip damage tensor, which represents this damage mode averaged over the RVE, turns out to depend on the average matrix crack length. In fact, it depends explicitly on the average COD, which in turn depends on the average crack length. The only surviving component of the slip damage tensor can be written as [59]

$$D^{\mathrm{sl}} = \frac{\pi^2 d^4 \eta^2}{64 v_{\mathrm{f}}^2} \langle c_{\mathrm{d}}^2 \rangle, \tag{12.15}$$

where d is the fiber diameter, v_{f} is the fiber volume fraction, and c_{d} is the COD; and the quantity within the brackets $\langle\,\rangle$ is averaged over the RVE volume.

Assuming the COD to be proportional to the crack length, (12.15) may be rewritten as

$$D^{\mathrm{sl}} = \xi \eta^2 \langle d^4 l^2 \rangle, \tag{12.16}$$

where ξ is a constant depending on the fiber volume fraction and fiber stiffness. The fiber diameter is placed within the brackets to allow for its variation. Equation (12.16) indicates that this damage mode depends directly and strongly on the fiber diameter in addition to depending on the matrix crack length, which in turn is expressible in terms of the fiber diameter, as in (12.7). Thus, the microstructural length scale in this case is the fiber diameter. Note that the fiber length over which sliding occurs is not a characteristic dimension of the mechanism when it occurs in conjunction with matrix cracking.

12.3.2 Ply Cracking in Laminates

Figure 12.9 shows an X-ray radiograph of a carbon–epoxy crossply laminate after being subjected to tension–tension cycling. In this 2D view, the horizontal lines are images of cracks in the 90° plies, while the vertical lines indicate cracks (also called *axial splits*) that lie in the 0° plies [27].

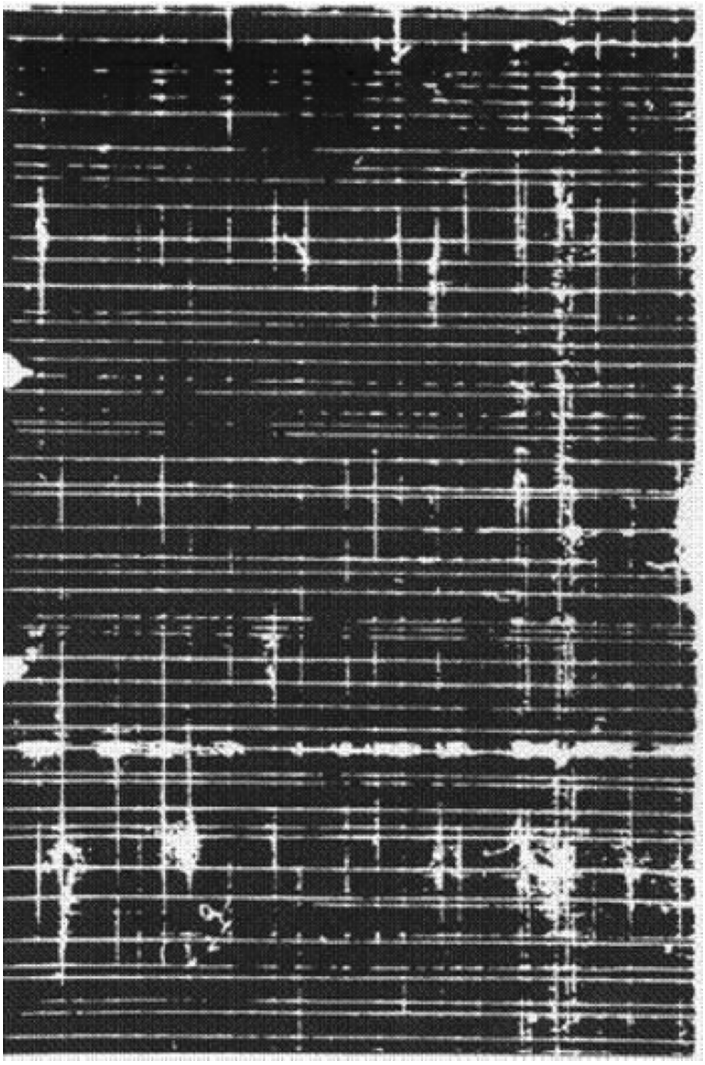

Fig. 12.9. An X-ray radiograph showing transverse cracks, axial cracks, and delaminations in a crossply laminate after fatigue [27]

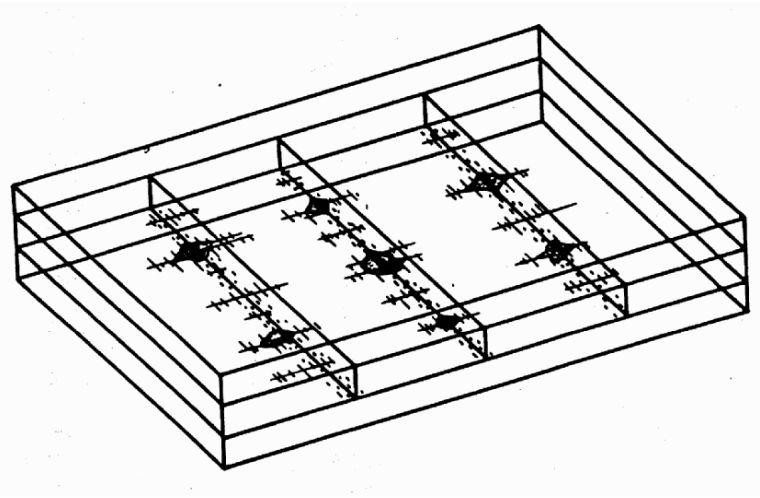

Fig. 12.10. The cracks and delaminations seen in the X-ray radiograph (see Fig. 12.9)

The shaded areas are sites of interlaminar cracks (delaminations), which are depicted in Fig. 12.10. For the sake of this discussion on length scales of damage, the focus will primarily be on ply cracking.

Figure 12.11 illustrates multiple matrix cracking in a ply of an arbitrary orientation θ with respect to the 90° direction. The cracks are shown at a mutual spacing s which represents the average crack spacing in an RVE. Using a second-order tensor characterization for this mode of damage [58] gives

$$D_{ij}^{\mathrm{pc}} = \frac{\kappa t_{\mathrm{c}}^2}{st\cos\theta} n_i n_j, \tag{12.17}$$

where the superscript pc stands for ply cracking, κ is a ply constraint parameter, t_{c} is the thickness of the cracked ply, and t is the laminate thickness. The components n_i of the unit vector normal on a crack surface are given by

$$n_i = (\cos\theta, \sin\theta, 0), \tag{12.18}$$

where θ, as shown in Fig. 12.11, is the crack inclination.

The laminate stiffness matrix in the presence of a fixed state of ply cracking is given by Talreja [58]

$$C_{pq} = C_{pq}^0 - C_{pq}^{\mathrm{D}}, \tag{12.19}$$

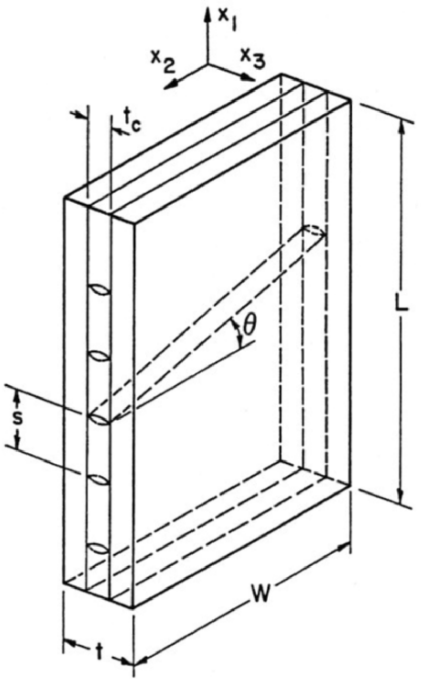

Fig. 12.11. Multiple cracking in a general off-axis ply of a laminate

where the indices p and q take values from 1 to 6 in accordance with the Voigt notation. The superscript 0 on the stiffness matrix indicates initial value while D indicates the contribution due to damage. Following classical laminate theory, the stiffness matrix for the virgin laminate can be written in terms of elastic moduli as below:

$$C^0_{pq} = \begin{bmatrix} \dfrac{E^0_1}{1-\nu^0_{12}\nu^0_{21}} & \dfrac{\nu^0_{12}E^0_2}{1-\nu^0_{12}\nu^0_{21}} & 0 \\ & \dfrac{E^0_2}{1-\nu^0_{12}\nu^0_{21}} & 0 \\ \text{Symm} & & G^0_{12} \end{bmatrix}. \tag{12.20}$$

The stiffness change due to damage depends upon the laminate ply layup. For instance, consider damage in $[0/\pm\theta_m/0_n]_s$ laminate. The ply cracks develop in $\pm\theta$ layers and the change in stiffness matrix is given as

$$C_{pq}^{\mathrm{D}}(\pm\theta) = C_{pq}^{\mathrm{D}}(+\theta) + C_{pq}^{\mathrm{D}}(-\theta) = \frac{\kappa_\theta t_{\mathrm{c}}^2}{st} \sin\theta \begin{bmatrix} 2a_1 & a_4 & 0 \\ & 2a_2 & 0 \\ \text{Symm} & & 2a_3 \end{bmatrix}, \quad (12.21)$$

where κ_θ is the constraint parameter for ply orientation equal to θ and a_i are phenomenological constants. For the particular case of damage in $[0/\pm\theta_m/0]_s$ laminates, the crack spacing in both $+\theta$ and $-\theta$ plies is assumed to be the same, as the damage response for both orientations would be nearly the same on external loading. Thus, these two damage modes, by virtue of their response behavior, effectively act like a single damage mode. Clearly, the above equation involves four unknown constants. These constants can be evaluated either experimentally or though numerical FE simulations. The procedure is outlined as follows. Experimentally observe degradation in stiffness properties for a reference laminate configuration such as a crossply laminate. Fit a straight line to the experimental data normalized with regard to stiffness of the virgin laminate. Evaluate $(C_{pq})_{\exp}$, i.e., compute E_1, E_2, υ_{12}, and $\upsilon_{21} = (E_2 / E_1)\upsilon_{12}$ at a certain crack spacing s_0. Using the equations above with $\theta = 90°$, the following is obtained

$$C_{pq} = (C_{pq})_{\exp} \Rightarrow$$

$$\begin{bmatrix} \frac{E_1^0}{1-\nu_{12}^0\nu_{21}^0} & \frac{\nu_{12}^0 E_2^0}{1-\nu_{12}^0\nu_{21}^0} & 0 \\ & \frac{E_2^0}{1-\nu_{12}^0\nu_{21}^0} & 0 \\ \text{Symm} & & G_{12}^0 \end{bmatrix} - \frac{\kappa_{90} t_{\mathrm{c}}^2}{s_0 t} \begin{bmatrix} 2a_1 & a_4 & 0 \\ & 2a_2 & 0 \\ \text{Symm} & & 2a_3 \end{bmatrix} = \begin{bmatrix} \frac{E_1}{1-\nu_{12}\nu_{21}} & \frac{\nu_{12}E_2}{1-\nu_{12}\nu_{21}} & 0 \\ & \frac{E_2}{1-\nu_{12}\nu_{21}} & 0 \\ \text{Symm} & & G_{12} \end{bmatrix}. \quad (12.22)$$

One important aspect pertaining to these constants is that though these constants are determined for the reference laminate, for other laminate configurations they are assumed to remain unaffected by angle θ for a given ply material. From experimental observations on carbon/epoxy [60] and glass/epoxy [68] laminates, this assumption is found to hold true. This is because the damage constants are primarily determined by the constituent ply properties and are not very dependent on ply orientation. Of course the influence of the ply orientation on the constraint posed by undamaged plies over damaged plies is important and is suitably carried by the "constraint parameter" κ through changes in COD.

The length scale variable entering the damage descriptor (12.17) and, consequently, the elastic response change (12.21) is the crack dimension, which for fully developed ply cracks, as assumed here, is the ply thickness t_c. The other crack dimension along the fiber axis in the ply extends as far as the imposed stress acts and is, therefore, not the characteristic length scale of the cracking mechanism. Expressed differently, the crack surface displacement, which is the cause of stress perturbations and, thereby, the elastic response changes, depends on the crack dimension through the ply thickness.

Although the ply cracks are assumed for simplicity to be sharp tipped, as illustrated in Fig. 12.11, in reality they must get blunted by merging with the local delamination, i.e., the separation of plies at the interface, caused by the intense stress field carried by the approaching ply crack fronts. The extent of the delamination cracks along the ply interfaces must depend on the interfacial bond strength as well as on the ply crack length t_c. In fact this situation is analogous to the fiber/matrix debonding in conjunction with matrix cracking in unidirectional CMCs, discussed previously. Drawing upon that analogy, it can be deduced that the delamination length enters the analysis not directly but via its ratio to the ply crack length t_c. Thus, once again, the relevant length scale variable is the total cracking ply thickness t_c.

When cracking occurs in more than one-ply orientation, multiple length scales result with each length scale variable equal to the combined thickness of the set of consecutive cracking plies of the corresponding orientation. Also, the delamination associated with each ply cracking contributes to the effect on the elastic response via the ratio of the associated delamination length to the ply crack length. Figure 12.12 illustrates the ply (matrix) cracking and delamination in an angle ply laminate.

Finally, return to the delamination mode observed in the fatigue of cross-ply laminates depicted in Figs. 12.9 and 12.10. As illustrated in Fig. 12.10, this delamination occurs locally at the intersection of cracks in the two orthogonal orientations in adjacent plies. The cause of this delamination and the effect of its presence have not been adequately analyzed. Therefore, any inference regarding its characteristic length scale is speculative at present. It appears, however, that the growth of the delamination is mainly along the two orthogonal ply crack directions, suggesting, therefore, two length scales. These length scales may be described as the two principal directions of an ellipse, which may be taken to approximate the delamination geometry.

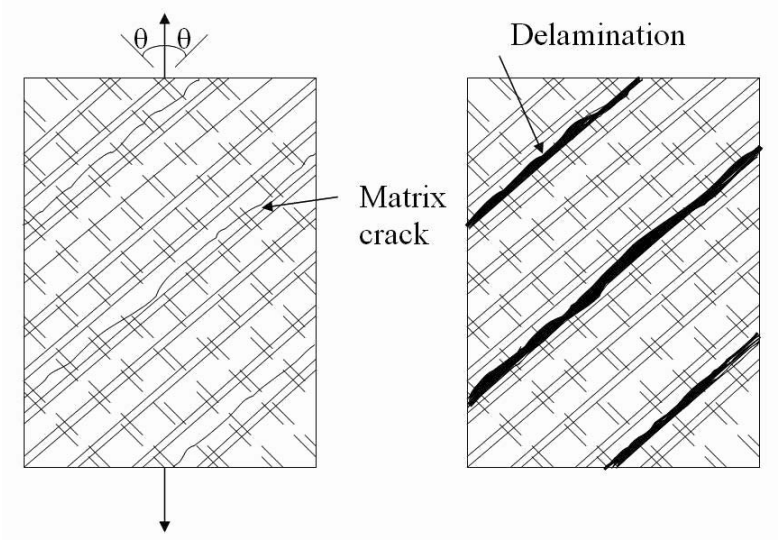

Fig. 12.12. Matrix cracks (*left*) and delamination (*right*) in an angle ply laminate

12.4 Multiscale Modeling of Damage for Elastic Response

12.4.1 Local vs. Nonlocal Description of Damage

The traditional way of describing the effect of damage entities on material behavior is quite similar to the definition of stress and strain, i.e., it is defined at a point by taking an infinitesimal volume around the point into consideration and taking a limit as volume goes to zero. However, this localized definition of damage is not consistent with the real behavior of the damage process. The damage entities affect the stress and strains in the neighborhood. Moreover, at the microscale level, the size of these damage entities, such as matrix cracks, debonds, etc., or flaws, such as voids, inclusions, etc., is finite and cannot be neglected. The third aspect to be considered is the variety of scales involved with different damage entities. The length scale aspects involved with different damage entities will be dealt with in Sect. 12.4.2.

The key aspect to be discussed here is the evolution of damage entities. A solid that is highly heterogeneous at the mesoscale is considered an effective homogeneous continuum at the macroscale. Macroscopic damage

variables are judiciously selected to reflect the effects of mesostructural-level irreversible processes on macroscale material behavior. Such damage descriptors are usually obtained through a "low-order" homogenization (spatial average) of individual damage entities, neglecting details of the distribution of damage throughout the RVE. Whereas effective moduli are somewhat insensitive to the distribution of microcracks, damage evolution is highly dependent on the local fluctuations in crack arrangement within the RVE used for stiffness calculations [32]. Bazant and Chen [5] discussed the scale dependence of energy release in fracture of heterogeneous, quasibrittle solids.

In the homogenization process, critical information regarding the largest flaw size, minimum distance between flaws, and distribution of damage within an RVE is irrevocably lost. Such information is crucial to the development of viable damage evolution equations. Current CDM approaches have been generally limited to the case of dilute (noninteracting) damage. This limitation suggests the need for a higher-order continuum description of damage that retains key aspects of the damage distribution within an RVE.

The choice of damage variable is either macroscopic or micromechanic based. The damage descriptors could be scalar or tensor, scalar descriptions being too simplistic in nature. In general, both macroscopically measurable and micromechanically inspired damage variables neglect the varying effects of nonlocal or "nearest neighbor" influences, e.g., shielding and enhancement associated with adjacent flaws, that are essential to formulate damage evolution laws. Inclusion of such effects represents, perhaps, one of the greatest challenges in the development of a robust CDM formulation. For these reasons, more careful consideration of appropriate ISV measures of damage is warranted.

The RVE is commonly defined as a cube of material with dimension L_{RVE} subject to the following conditions [34, 35]

$$\begin{aligned} &\frac{d}{L_{\mathrm{RVE}}} \ll 1, \quad L_{\mathrm{c}} \le L_{\mathrm{RVE}} \le L, \\ &\left|\frac{\partial \sigma_{ij}}{\partial x_k}\right| L_{\mathrm{RVE}} \ll \sigma_{ij}^{0}. \end{aligned} \tag{12.23}$$

where d is the characteristic size of microconstituents, L_{c} is the heterogeneity correlation length, L is a characteristic macroscopic structural dimension, σ_0 is the mean field (volume averaged) stress, and x_k (x_1, x_2, x_3)

are the components of a Cartesian basis. Statistical homogeneity, for general purposes, requires that all response functions of interest at the scale of the observation volume window (Helmholtz free energy, Cauchy stress tensor, stiffness tensor, etc.) are essentially invariant with respect to window position [36]. It is very important to properly select suitable observation windows for averaging response functions and to analyze the influence of observation window boundary conditions, e.g., uniform vs. "random-periodic" traction and displacement boundary conditions, on the statistical homogeneity of response functions for a given window size. Due to multiple scales involved with evolving damage mechanisms,

$$\mathrm{RVE}_{\mathrm{evolution}} \neq \mathrm{RVE}_{\mathrm{stiffness}}. \tag{12.24}$$

For further discussion on RVE-level damage characterization, the reader is referred to [36].

12.4.2 Microstructural Length Scales

In Sect. 12.3, the governing dimensions of the damage entities are examined from the viewpoint of elastic response in the presence of damage. Two specific cases of damage in unidirectional CMCs and PMC laminates have been examined. The framework within which the issue of characteristic lengths has been analyzed is CDM using characterization of damage with second-order tensors. This particular representation of damage, in the form used here, provides a consistent characterization of the basic damage entity involved in each case, e.g., a matrix crack in a CMC and a ply crack in a PMC laminate.

The crux of the characterization is the "influence" vector, which provides a relevant measure of the action induced by the presence of the damage entity. By expressing the magnitude of this vector in terms of the characteristic and governing dimension of the damage entity, the "essence" of the damage entity is carried into the damage entity tensor. This dimension, when properly identified and related to the microstructural entities, provides the length scale associated with the damage mechanism considered.

The relevance of the length scale to determining the elastic response affected by that damage mode becomes clear when the response measured over the RVE is examined. For this, a damage mode tensor, which acts as an ISV in a continuum damage framework, is considered. The damage mode tensor has been examined in a simple form, such as that in (12.10), which is the volume average of the damage entity tensor over the RVE.

This does not account for the damage entity distribution and can, therefore, be used only for the RVE-averaged, i.e., the mesoscale, response and not for describing damage evolution. Thus, the length scales of damage within the context of the elastic response have been examined.

The next question to address is: What is the significance of the length scales of damage? The basic concept behind length scales appears to be the intuitive idea that effects seen at a given observation "window," e.g., RVE size, must be determined by events occurring at dimensions smaller than the window size. Implicit is the assumption that those events are associated with certain discrete entities, such as grains in a polycrystalline material, and that the action of those entities and interactions between them, when averaged over the window size, provides the "response" variables applicable at that scale.

Carrying this logic one step "behind" would suggest that the response at the scale of the discrete entities in an RVE could be given by the subentities lying within those entities. Thus, if a grain is viewed as an entity, then the dislocations within the grain could be the subentities. This move to smaller and smaller size scales could, in principle, have no end other than the limit set by the tools of observation and analysis available at a given time.

In engineering science, in contrast to "pure" sciences, one takes a pragmatic approach driven by the application or need at hand. From this point of view, one must consider the purpose first and go as far down in scales as needed. Thus, if the purpose is to determine the elastic response changes induced by damage in a composite material, then one must go as much down in length scales as necessary to determine the reversible deformation (or stress) related effects but no further.

The next question is whether a hierarchy of length scales can be identified. What has been illustrated by the discussion of the two cases of composites with damage is that a simple hierarchy of length scales does not exist. Instead, a complex damage mode may involve more than one governing length, e.g., the matrix crack length and the interfacial sliding length for a fiber-bridged crack. Also, multiple damage modes may operate simultaneously and interactively, leading to multiple length scales, e.g., in the case of multiple off-axis plies in a laminate. These considerations suggest that an alternative is needed to the strategy of starting at the smallest length scale and working up the scale hierarchy. Talreja [60] proposed one such strategy, the so-called "synergistic" damage mechanics. The following discussion will address the two strategies.

12.4.3 Hierarchical Multiscale Modeling

There are three levels of modeling of composites with a hierarchical approach, as depicted in Fig. 12.13:

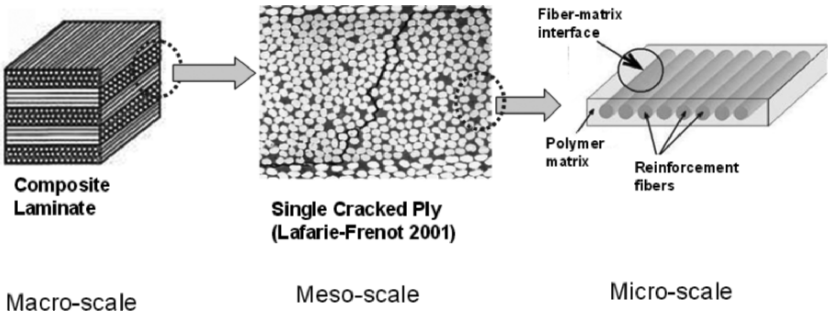

Fig. 12.13. Three scales involved in hierarchical modeling of composite laminates

- *Microscopic level*. This is the lowest level of observation, wherein fiber and matrix phases are modeled separately and the average properties of a single reinforced layer are determined from individual constituent properties by a suitable homogenization technique. With regard to damage in composites, micromechanics includes matrix cracks inside a layer, called *microdamage mechanics* (MDM). Hashin type of analyses belongs to the set of MDM approaches.
- *Mesolevel*. At this level, the ply is considered homogeneous and the virgin (undamaged) material is regarded as either orthrotropic or transversely isotropic. This scale is very useful in describing and predicting the damage/failure of composites.
- *Macroscopic level*. This refers to the structural level wherein the whole structure is considered as a homogeneous continuum and material behavior is described by an anisotropic constitutive law. The traditional concepts of continuum mechanics work quite remarkably here; and, thus, the overall structural behavior to external loading can be studied using suitable FE modeling or by solving a boundary value problem with effective material properties.

It would be fair to say at the outset that the hierarchical multiscale approach is intuitively logical. For a complex composite architecture, which is quite often the case in practical applications, one can think of starting

with the smallest basic unit – a discrete fiber embedded in a matrix – and proceed to the level of a representative unit of a collective fiber arrangement. The basic unit can be analyzed as a piecewise homogeneous continuum, with two regions, if fiber and matrix are considered, or three, if an interfacial layer is added. The result (stress, strain, temperature, etc.) can then be averaged in some sense over a representative unit to get a description for the homogenized medium. Several models for doing this exist, e.g., the Mori–Tanaka method. These models aim at bridging the two scales: the scale of the basic unit and the RVE scale.

Generally, the issue of uniqueness remains unresolved in the sense of representation of the collective fiber effect. There is as yet no precise and rigorous definition of a representative unit for a general case, which is the source of the lack of uniqueness. A logical extension of the discrete-to-collective bridging of the fiber–matrix case to higher scales produces the hierarchical approach in multiscale modeling. One can argue whether or not this approach is efficient, in spite of its logic. Historically, the hierarchical approach has not preceded other approaches. A structural analyst has worked with macrolevel descriptions of material behavior, e.g., the classical laminate plate theory, and has looked for microlevel information as needed. A materials developer, on the other hand, has focused on effects of constituents and their microstructural arrangements on properties. In recent years, the seemingly abundant computer power has motivated the hierarchical approach with the hope of integrating materials design and structural analysis.

The objective here is to examine approaches for multiscale analysis of damage in composites. A first thought would be to conduct damage initiation and progression analysis as a part of the hierarchical multiscale approach. It turns out not to be that straightforward. The issues confronting this approach are discussed below, along with the merits of an alternative approach.

An overall view of the multiscale approach is reviewed first. Figure 12.14 illustrates, from left, an object of structural integrity assessment within which a region of potential criticality (failure) exists. This region (a substructure) is analyzed to determine the loading on its boundary. The next step is to examine how this loading induces damage. This step requires analyzing heterogeneities (microstructure, generally), which govern initiation of damage. Simple examples are debonding of fibers from the matrix and matrix cracking from broken fiber ends. The analysis of local stress/strain fields to determine such microfailures is commonly referred to as *micromechanics*. Micromechanics could be conducted at multiple scales. An example is fiber/matrix debonding at the fiber diameter scale and coalescence of the debond cracks at the scale of a representative number of fibers.

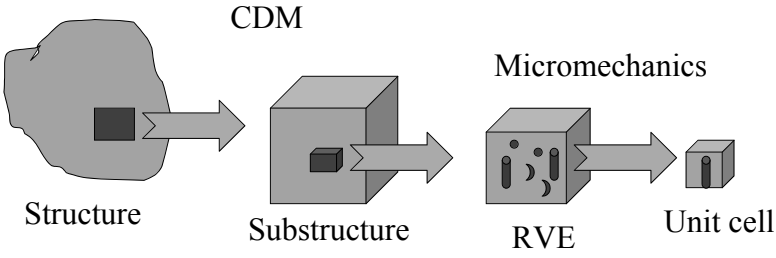

Fig. 12.14. A multiscale approach starting from the structural scale, moving down to lower scales

In Fig. 12.14, the direction of the arrows indicates moving from the structural (macro) scale downward to decreasing length scales. Until the microstructural entities are explicitly included in an analysis, the regime of analysis is characterized as "continuum," beyond which it is known as micromechanics. In the context of damage, the continuum regime is called *continuum damage mechanics*, while the micromechanics is typically not given an additional characterization (except, perhaps, occasionally as micro-damage mechanics) [23].

Historically, the fields of CDM and micromechanics have developed independently, CDM going back to [31], while micromechanics originated in various works; but its characterization as a coherent field may be credited to Budiansky [6], who defined it as "the mechanics of very small things." In recent years, the upsurge of computational mechanics has also boosted micromechanics, adding the aspects of numerical simulation and length scale-based characterizations such as "nanomechanics."

The increasing confidence in the power of computation has led to the notion of the hierarchical approach, with the implicit assumption that "basic" laws, when placed into a simulation scheme, will lead to physically correct results. Thus, once the microstructure, at any chosen level of length scale, has been codified in a simulation scheme, the results of the computation will describe the behavior at the next higher level, the assumption goes. In the context of damage mechanics, this may raise a few issues, as discussed below.

The first issue in a hierarchical approach is the choice of length scales. As discussed in Sect. 12.3, the microstructural length scales are relatively straightforward; and, consequently, setting up a hierarchy of scales and procedures for bridging between them can be accomplished relatively easily. However, the *microstructural configuration and driving forces for damage initiation and progression determine the length scales of damage*.

Thus, length scales of damage and their hierarchy are not fixed but are subject to evolution. To illustrate this, consider ply cracking in a laminate. In the early stage, individual ply cracks initiate from debonding of fibers, giving the damage length scale in terms of the fiber diameter. When the ply cracks are fully grown through the ply thickness, the mechanism of interest is the multiplication of cracks. At this stage, the damage length scale is crack spacing, which in turn depends on the ply thickness as well as the constraint to surface displacement of the ply cracks. The two-stage behavior and the evolving nature of damage complicate any hierarchical scheme for predicting response.

Another issue in a hierarchical approach is the multiplicity of damage modes. If more than one damage mode operates at a time and there is interaction between the modes, then a hierarchy of length scales becomes questionable. Consider ply cracking in a commonly used quasi-isotropic $[0/\pm 45/90]_s$ laminate in axial tension. Multiple matrix cracking occurs in 90° plies, followed by the same in plies of –45° and 45° orientations. The three-ply cracking modes progress interactively and, at some stage, concurrently. The length scales associated with the three damage modes do not show hierarchy. Consequently, bridging the scales by some averaging scheme becomes irrelevant. Further complicating the hierarchical scale arrangement is the interlaminar cracking that results from the cracking in individual off-axis plies.

12.4.4 Synergistic Multiscale Modeling

An alternative to the hierarchical approach is the SDM approach proposed by Talreja [60]. Conceptually, the approach combines the strengths of CDM and MDM. In CDM, the material microstructure, e.g., distributed fibers, and the distributed damage, which may be called the *microdamage structure*, are treated as smeared-out fields. This homogenization is illustrated in Fig. 12.15 as a two-step process, where the material microstructure is viewed as consisting of "stationary" entities, e.g., fibers and plies, and the micro-damage structure is considered as a family of evolving entities, e.g., cracks and voids. A set of response functions are expressed in terms of the field variables (stress, strain, and temperature) and internal variables, which represent the smeared-out field of evolving damage entities. The internal variables, although being field quantities, actually have an RVE associated with them at each material point. Strictly speaking, there is another RVE associated with the stationary microstructure; but it is customary in continuum treatments to bypass it by requiring that the quantities, such as the elastic moduli of virgin material, be measured at a scale much larger than the

scale of the individual stationary microstructure entities. There is a tendency to do that for the RVE associated with damage as well, as evidenced in finite element-based analyses where reduced (damage induced) properties are assigned at nodal points. The reduced properties are meaningful only at the RVE scale, which depends on the length scales of damage discussed above.

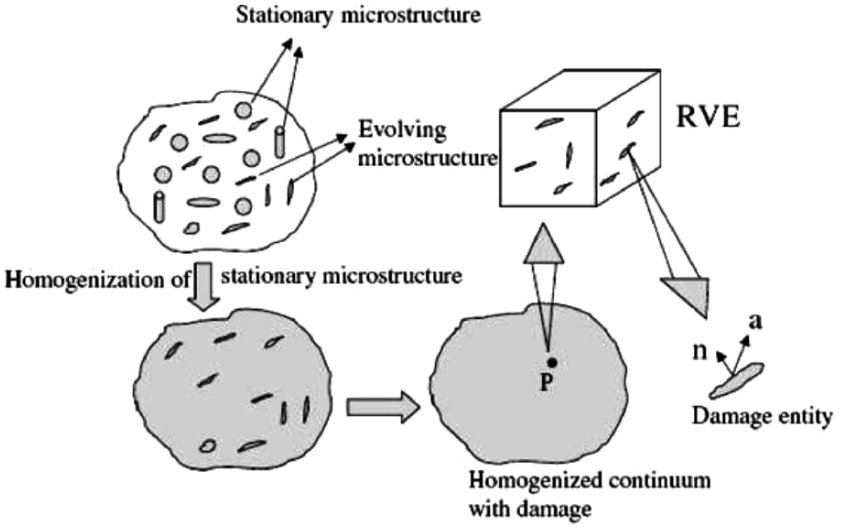

Fig. 12.15. The two-step homogenization process for composites with damage

Although the hierarchical approach seems to be the most common choice, it disregards many of underlying issues. Another suitable approach is to combine the micromechanics with continuum damage mechanics, called *synergistic damage mechanics* [60]. To illustrate the structure of SDM, consider the Helmholtz free energy function for isothermal mechanical response as

$$\phi = f(\varepsilon, D), \tag{12.25}$$

where the strain tensor ε and damage variable D, generally also a tensor, are independent variables representing the material state. The variable D is viewed as an internal variable, representing some measure of the collective presence of damage entities in an RVE at the considered point where the material response is sought. In Fig. 12.15, the RVE at a point is shown as a finite-sized cube of material containing a representative sample of damage entities.

The internal state (damage) in a general case may contain multiple modes, such as the ply cracking modes in a $[0/\pm45/90]_s$ laminate. In the

conventional CDM approach, the response function R, and any function derived from it, is expressed in terms of D, which is formulated to represent a measure of the intensity of damage. Examples of such measures are void volume fraction and crack number density. Such "passive" measures end the CDM at the RVE level, i.e., the role of CDM gets limited to generating constitutive relationships at the RVE (meso) level that are then used for analyzing structural (macro) response. In the SDM approach, one proceeds down from the RVE level to one or more microlevels as warranted by the situation at hand. This is accomplished by developing a characterization of damage entities that is "active" in the sense that the presence of damage entities is accounted for by including the "influence" of damage entities.

In contrast, the passive characterization is limited to only accounting for the "presence" of damage entities by measures such as crack number density, as noted above. The characterization of influence is accomplished by assigning a two-vector representation to a damage entity, as illustrated in Fig. 12.15. The vector a carries the influence through its magnitude and direction. The magnitude of the vector represents a measure of how much the damage entity is able to affect its surroundings, while the direction of the vector indicates the orientation in which this effect acts. For instance, if there is concern about the deformational response of a composite, then clearly the surface of a given damage entity must conduct a displacement to affect this response. Imagine, for instance, a transverse crack in 90° plies of a $[0/\pm45/90]_s$ laminate. The degree to which this crack opens under an imposed axial load increment will determine how much the axial elastic modulus of the composite will reduce. If the axial stiffness of the sublaminate $[0/\pm45]$ is high, then the COD will be low; and, consequently, the modulus reduction will be small. In a passive damage characterization, where only the crack number density enters, no distinction can be made between the presence of cracks in different constraining environments.

In the SDM approach, the constraint to the damage entity influence is represented in a constraint parameter, such as α in (12.8) for a fiber-bridged matrix crack. The determination of the constraint parameter, and generally any influence function, is accomplished by a micromechanics analysis at levels warranted by the length scales of damage.

The SDM approach has been illustrated in [69] for the elastic response of $[\pm\theta/90_4]_s$ laminates and in [70] for the linear viscoelastic response of crossply laminates of different 0/90° ply mix. In each case, the transverse cracking in 90° plies was considered as the damage mode subjected to different constraints. Thus, in the $[\pm\theta/90_4]_s$ laminates, θ is varied to vary the constraint, while no cracking is considered in the $\pm\theta$ plies. The objective in both of the works just cited was to demonstrate SDM for the case of one

damage mode with varying constraint and varying mesoscale (RVE size). This addresses the first of the two issues in the hierarchical multiscale modeling discussed previously. This author and his associates in ongoing work are treating the other issue of multiple damage modes. The main ideas in dealing with the first issue are discussed next.

Let us consider the elastic response of $[\pm\theta/90_4]_s$ laminates. At a damage state where multiple transverse cracks of average spacing s exist, an elasticity response function (modulus) derived from the free energy function (12.25) can be expressed as [56]

$$\frac{R}{R_0} = 1 - \kappa \frac{t_c}{s} f_1 f_2, \tag{12.26}$$

where R_0 is the initial (undamaged) value of the response, t_c is the thickness of the cracked plies, κ is the constraint parameter, and f_1 and f_2 are normalized functions of the laminate geometry (ratio of cracked to uncracked plies) and ply properties, respectively. The expression in (12.26) results from a linearized theory; more terms of higher order in t_c / s will appear in a higher-order theory. In [69], it was shown, based on MDM analysis, that the constraint parameter κ could be approximated as a function of θ by a polynomial function of ply properties and ratio of thicknesses of cracked and uncracked (constraining) plies. Thus, with input from MDM, the CDM framework could be applied to the class of $[\pm\theta/90_4]_s$ laminates. Note that, in the conventional CDM framework, the response function R must be calculated separately for each θ value.

In the case of linear viscoelastic response, R, κ, f_1, and f_2 are all functions of time. In [70], it was shown that the functions f_1 and f_2 are normalized functions of laminate geometry and relaxation moduli of undamaged plies, respectively, while the time variation of κ was found by parametric studies of $[0/90_n]_s$ to be given by a polynomial function of the ratio of axial relaxation moduli of the cracked plies to that of the uncracked plies. Once again, an MDM analysis allowed predicting viscoelastic response (for a fixed crack density) for a class of composites with a CDM framework without experimentally determining material constants for each laminate configuration.

12.4.5 Multiple Damage Modes

The authors are presently working toward developing SDM methodology for multiple damage modes. The multiple damage modes may appear due

to separate damage mechanisms, such as matrix cracks, debonding, delaminations, etc. Alternatively, if the matrix cracks appear in more than one orientation, these can also be treated through multiple damage modes by assigning one damage tensor to cracks of a particular orientation. SDM methodology has been successfully used to predict stiffness degradation due to matrix cracking in laminate configuration. Work is ongoing to predict damage behavior for more general laminate layups. Based on the results available for the case of multimode damage using SDM, it is evident that a purely MDM approach or a conventional CDM framework will not provide results without excessive computation (for MDM) or tedious experiments (for CDM). Section 12.4.6 presents some of the recent advances pertaining to the SDM approach.

12.4.6 SDM Characterization of Damage in Off-Axis Plies

In the case of ply cracking, the most direct measure of damage is the separation of crack surfaces, known as *crack opening displacement*. These surface displacements do not occur freely due to the constraints from the adjoining undamaged plies. These "constraint effects" are suitably incorporated in the CDM formulation through the constraint parameter κ. Using COD, there are four common ways to characterize damage in the laminates:

1. *MDM/micromechanics*. For a given laminate system, the ply cracks inside the RVE can be characterized by defining an equivalent boundary value problem; and its solution would yield expression for COD in terms of laminate geometry and material properties. This type of analysis has been performed [66] for crossply laminates. This methodology yields exact bounds on stiffness degradation due to ply cracking. Unfortunately, it is limited to only crossply laminates. Solving a boundary value problem for off-axis plies is impossible due to too many unknowns in the formulation.
2. *Gudmundson model*. The second approach is to use the Gudmundson model [16] in which he characterized damage using average COD. Although the stiffness degradation relations are quite accurate in this model, the COD is calculated assuming a system of infinite cracks in a homogeneous medium. Hence, it does not include the "constraint effects" of the adjoining undamaged plies.
3. *Hierarchical approach*. This approach solves the boundary value problem inside RVE using FE simulation and then integrates it to the higher scale to obtain the overall macrolevel response of the structure. This methodology can be used to solve any laminate

layup and looks quite straightforward but has important limitations, which have already been discussed in detail.

4. *Synergistic damage mechanics*. SDM follows the regular CDM formulation except that the constraint effects area is evaluated using numerical simulations at the micromechanics level. This approach can be applied to a variety of laminate layups. It captures the physics of dissipating mechanisms in an accurate manner and is more computationally efficient than MDM or the hierarchical approach. It can also include the multiscale nature of damage efficiently and can solve problems involving multiple damage modes. In the following paragraphs, its applicability to characterize damage in off-axis plies is described.

The procedure for analyzing damage behavior in off-axis plies using SDM methodology is explained in Fig. 12.16. The example illustrated here is of damage in $[0/\pm\theta_4/0_{1/2}]_s$ laminates. The approach needs both micromechanics and CDM for a complete evaluation of structural response.

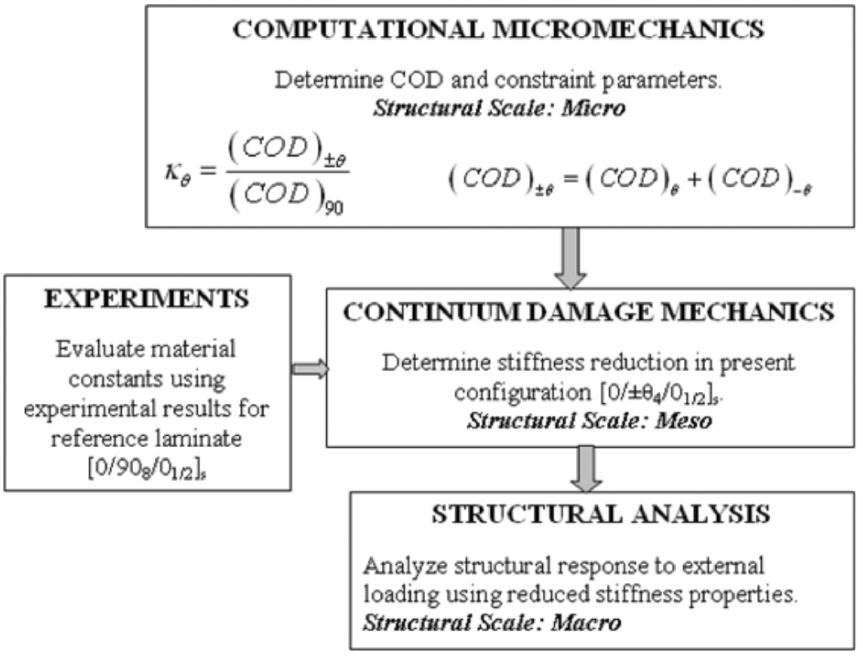

Fig. 12.16. Flowchart showing the synergistic multiscale methodology for analyzing damage behavior in a general symmetric laminate $[0/\theta_1/\theta_2]_s$ with matrix cracks in multiple orientations. The example taken here is $[0/\pm\theta_4/0_{1/2}]_s$ laminate with transverse matrix cracks in and $+\theta$ and $-\theta$ plies

Micromechanics involves analysis over a unit cell (or RVE) to determine COD values and the constraint effect due to adjoining uncracked plies. These constraint effects are carried over in CDM formulation through the "constraint parameter" κ. In a separate step, the material constants a_i appearing in expressions for damaged laminate stiffness relationships are determined from data for a reference laminate, such as $[0/90_8/0_{1/2}]_s$ for the present study. CDM expressions, given in (12.19), are then employed to predict stiffness degradation with crack density. The subsequent structural behavior in response to external loading is analyzed through a suitable FE model with material input as degraded stiffness properties at a given crack density (or corresponding applied strain).

To evaluate the constraint effect of undamaged plies over damaged plies, detailed 3D FE analyses over RVE, as shown in Fig. 12.17, were performed for angles, θ = 25°, 40°, 55°, 70°, and 90°. Specifically, CODs were determined as a function of ply orientation, ply thickness, and stiffness ratio of constrained to cracked plies. In literature, many analyses can be found which use 2D generalized FE models even for analyzing damage in off-axis laminates, e.g., $[0/90/\pm45]_s$ laminates [63]. However, a 2D FE modeling may not be accurate for analyzing structural behavior when damage is present in multiple modes as different sections in the width direction no longer behave in a similar manner. Only the key results are presented here.

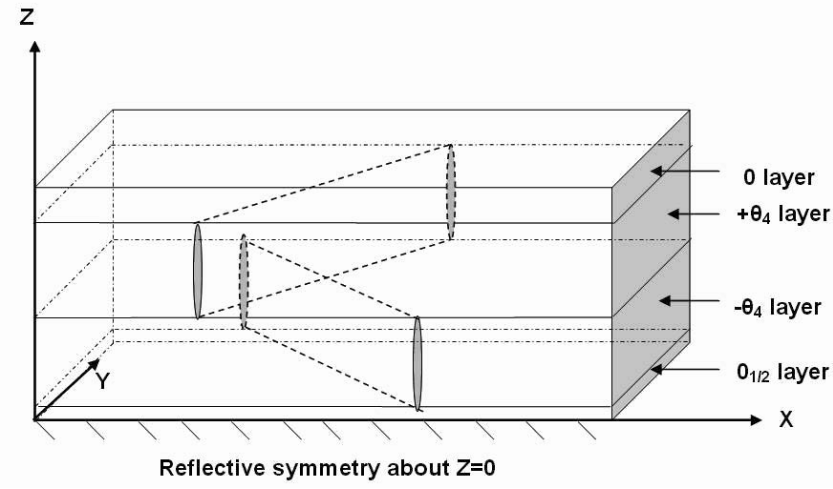

Fig. 12.17. A representative unit cell for $[0/\pm\theta_4/0_{1/2}]_s$ laminate configuration used in FE modeling. This shows the symmetry about the laminate midplane as the laminate is symmetric

Figure 12.18 shows the comparison between the experimental results and the 3D FE analysis for COD values evaluated at 0.5% axial strain. The FE results match very well with the experimental values. The experimental results are already published in [65, 66]. The experimental values are shown for ply orientations greater than 40° as there were no surface cracks observed below this angle. Average COD increases with ply orientation, but the rate of increase decreases and almost flattens out for crossply laminates ($\theta = 90°$). Thus, the effect of damage due to transverse matrix cracking is substantially lower in off-axis plies than in crossply laminates. This illustrates one advantage of using off-axis laminates, especially in complex loading. The profile of the crack opening was observed to be similar to that of a single crack in an infinite isotropic elastic medium subjected to a uniform far-field stress. The constraint due to adjoining plies makes it somewhat flat.

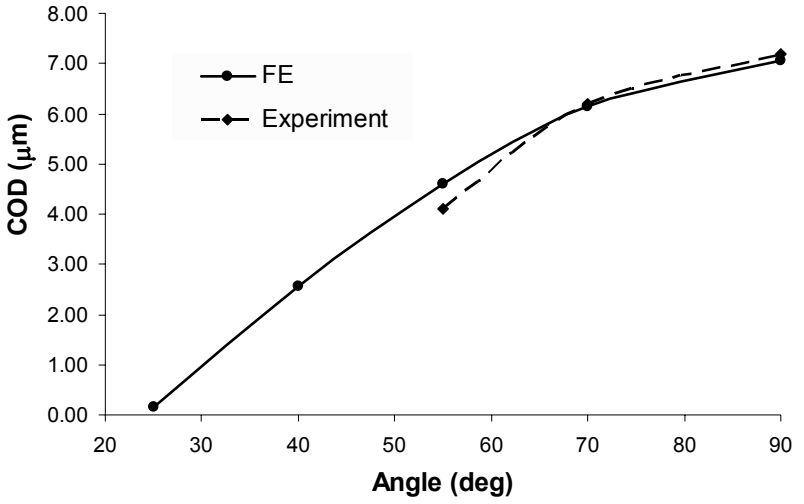

Fig. 12.18. Comparison of average crack opening displacements with experimental results for $[0/\pm\theta_4/0_{1/2}]_s$ laminate for $\varepsilon_{axial} = 0.5\%$

To understand the constraint effects further, a parametric study was performed by varying the stiffness of the constraining plies; and its effect on COD was analyzed. Figure 12.19 shows the effect of stiffness ratio on the COD of crack $\pm\theta$ plies. The COD values are normalized with the thickness of the cracked layer. For all cracked-ply orientations, normalized COD decreases as the constraining plies become stiffer than the cracked plies. The normalized COD values can be fitted to the following power law

$$\Delta\overline{u}_y = A + B\left(\frac{E_x^{\pm\theta}}{E_x^{90}}\right)^{-n}, \tag{12.27}$$

where A, B, and n are the constants determined from the FE simulations, $E_x^{\pm\theta}$ represents the elasticity modulus of $\pm\theta$ plies in the laminate longitudinal direction, and the corresponding elasticity modulus of 90° ply in the longitudinal direction. The effects of ply thickness over CODs were also studied. To evaluate the stiffness degradation, the damage constants appearing in (12.21) were evaluated based on experimental plots for the reference laminate $[0/90_8/0_{1/2}]_s$. Figure 12.20 shows the plot of predicted longitudinal Young's modulus and Poisson's ratio normalized by their virgin state (undamaged) values with respect to the crack density for $\theta = 70°$. The stiffness reduction in laminates with damage in off-axis plies is found to be less significant than in damage in crossply laminates.

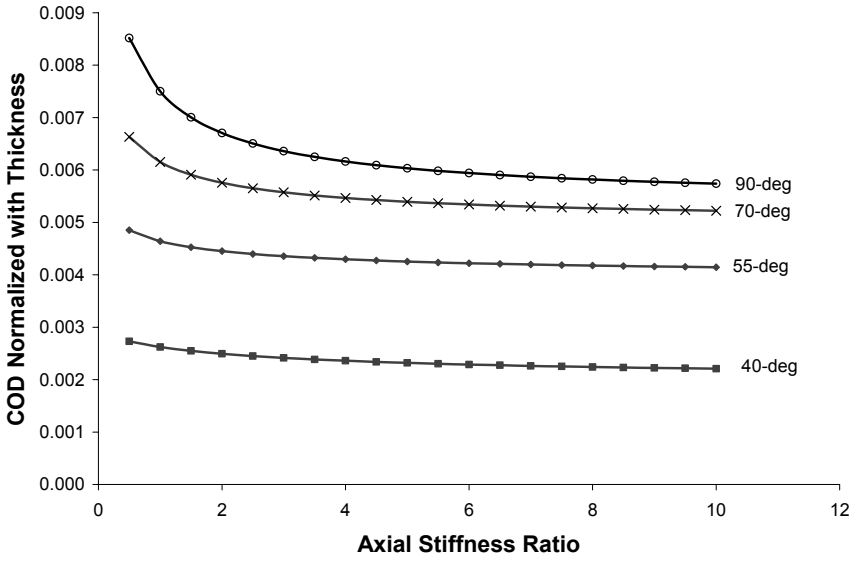

Fig. 12.19. Variation of COD for $[0/\pm\theta_n/0_{1/2}]_s$ laminate with axial stiffness ratio

To expand the scope of the SDM application, the authors are currently studying the damage behavior in $[0_m/\pm\theta_n/90_p]_s$ laminates, which involves matrix cracks in three different orientations and is characterized using CDM formulation with a separate damage mode tensor for each orientation. This will be taken up in a future publication.

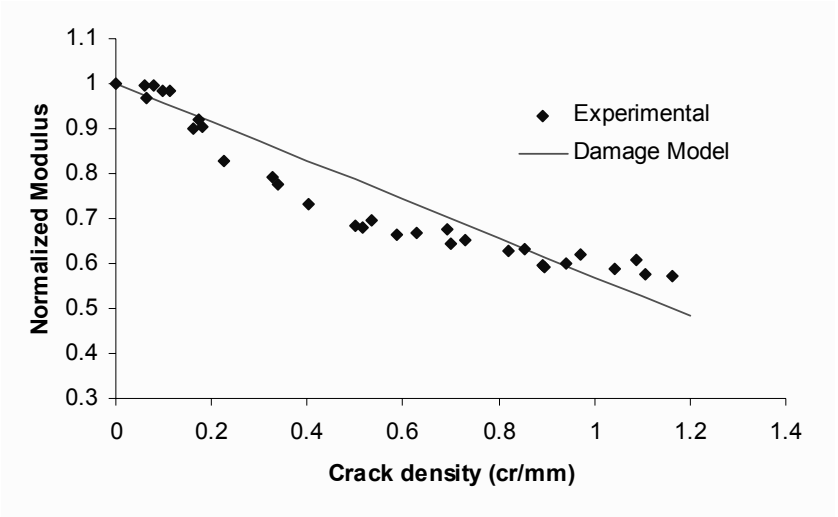

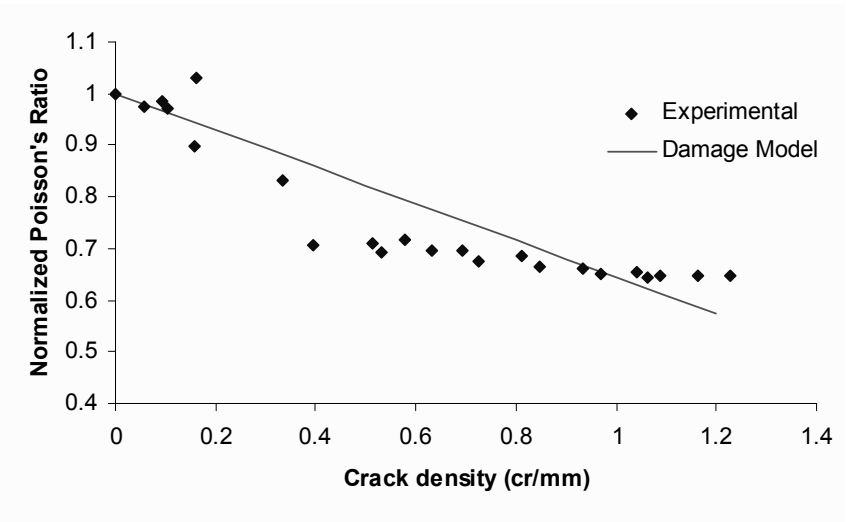

Fig. 12.20. Predicted stiffness reduction for $[0/\pm 70_4/0_{1/2}]_s$ laminate compared with experimental results

12.5 Structural Integrity and Durability Assessment

In composite damage modeling and engineering research generally, it is important to have the ultimate goal in mind to develop the right strategy

and to be clear about the context. For the authors, the goal is to assess integrity and durability of composite structures. This goal is not new; it has been in sight for most individuals involved in materials modeling. Figure 12.21 shows the "big picture" in which structural integrity and durability assessment are embedded. The starting place in the iterative process illustrated in the figure is manufacturing. One selects a process, e.g., liquid compression molding, and quantifies its process parameters, which along with other manufacturing details involved, such as machining and assembly, determine the material state in the component manufactured. The material state is characterized by a set of properties, e.g., elastic moduli, strength, and fracture toughness. These properties undergo evolution in the service environment due to phenomena such as fatigue, creep/viscoelasticity, and aging. The performance evaluation for the expected component life involves assessment of structural integrity and durability. Finally, a tradeoff study of cost against performance is conducted to assess the cost effectiveness. Most cost drivers lie in the manufacturing process, whose parameter variation allows moving toward the optimal design.

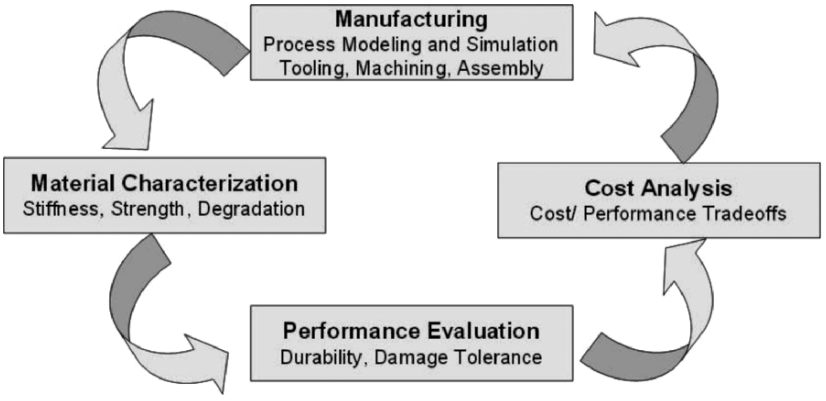

Fig. 12.21. The "big picture" considerations for cost-effective design of composite structures

Returning to the structural integrity and durability assessment, the role of materials modeling for composites is described in Fig. 12.22. Here the starting place is structural stress analysis of a given component, often by a finite element code. The input to this is the loading environment along with a deformational model, which is taken to be that of the initial material state (as produced by the manufacturing process). In most cases, prior

experience guides in identifying critical sites in the component that are prone to failure. The local stress states in those sites determine the initiation and evolution of damage, also called *subcritical failure*. The mechanisms of damage depend additionally on the "microstructure," i.e., the fiber architecture, ply configuration, fiber/matrix interface, etc. In the discussion above, two cases of damage have been covered in two widely different microstructure scenarios. Along with this, the damage mechanics approaches, CDM and MDM, have been discussed as well as the hierarchical vs. SDM strategies. The outputs of these modeling efforts are either deformational changes, expressed as stiffness–damage relationships, or strength (failure criticality) or both. The stiffness change result also provides incremental input to the stress analysis, updating the deformational model. The final goal of life prediction (durability) can be reached by either a stiffness criterion or a strength criterion, depending on the performance requirement.

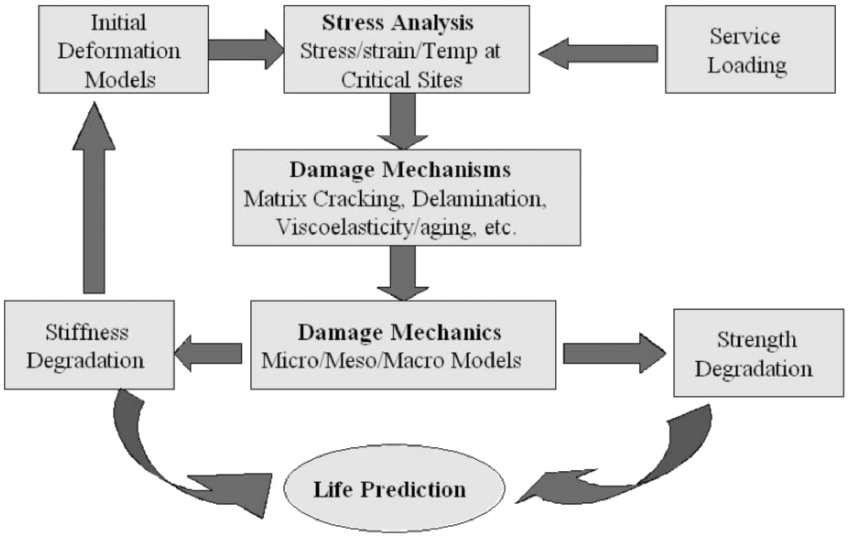

Fig. 12.22. Integrity and durability assessment procedure for composite structures

The multiscale modeling approach discussed here has been focused on the deformational response. Other considerations are needed for treating the local-to-global failure. The length scale issues are substantially different for failure than for deformational response. Discussion of these calls for a separate, focused treatment is reserved for a future work.

12.6 Conclusions

Multiscale modeling of composite materials generally, and of damage in these materials particularly, is still in the early stages of development. The overall field of multiscale modeling is undergoing intense development and is strongly driven by efforts to uncover phenomena that do not seem to be amenable to analytical treatments or are not yet feasible to study by direct or indirect observation. The need to enrich structural-level modeling with details of lower scales at which physical mechanisms operate forms a part of the multiscale modeling field. The discussion offered here has been targeted at this part.

The objectives of structural-level analysis of composites undergoing damage are to determine deformational response and assess structural integrity and durability. The treatment above has attempted to make the case that starting at a small scale, such as the fiber diameter, and working up the scales to the structural level is not an effective way to meet these objectives. This so-called *hierarchical multiscale strategy* will not, on its own, produce the observed features of damage, such as multiple cracking and multiple modes of multiple cracking. As discussed above, the characteristic scales change from a single damage entity to a damage mode and from a single damage mode to multiple damage modes. Furthermore, the length scales in each damage mode evolve as damage progresses, rendering the hierarchical approach a frustrating exercise. It should be realized that efforts in hierarchical multiscale modeling usually address phenomena at one scale and seek their outcome in terms of parameters valid at the next higher scale. In principle, of course, such efforts can be expanded to address multiple evolving scales, but it does not appear to lead to an effective strategy. Once again, this assessment is in the context of the set ultimate objective of analyzing behavior at the structural level.

An alternative strategy is to take the approach advocated here as SDM. In this approach, one begins at the structural level, i.e., the macrolevel, and formulates the material response in terms suited for structural analysis, e.g., by a finite element method. The scale at which the material response is addressed, i.e., the scale over which averaging is performed to determine the response functions, is the scale of an RVE, also called the *mesoscale*. The choice of the mesoscale is determined by the operating damage modes, which are known from experimental observations. In new situations, where experiments may not be feasible, a separate numerical simulation may be performed to uncover damage modes. In any case, the idea is not to indulge in an indiscriminate microlevel simulation but specifically to seek information needed at the mesolevel, as dictated by the macrolevel formulation.

In the examples discussed above, the relevant information is the crack surface displacement as affected by constraints of the material surrounding a crack in the mesolevel volume.

If the field of multiscale modeling is to advance beyond academic interests, it must address practical structures. Practical composite structures are manufactured by techniques that inevitably introduce defects such as voids in matrix, misaligned fibers, and interfacial disbonds. A multiscale modeling strategy must incorporate such defects in a judicial manner without increasing complexity to an impractical level. Work along these lines is ongoing in the authors' research group and will be reported as it progresses.

References

1. Allen DH, Harris CE, Groves SE (1987) A thermomechanical constitutive theory for elastic composites with distributed damage. I. Theoretical development. Int J Solids Struct 23:1301–1318
2. Allen DH, Harris CE, Groves SE (1987) A thermomechanical constitutive theory for elastic composites with distributed damage. II. Application to matrix cracking in laminated composites. Int J Solids Struct 23:1319–1338
3. Argon A (1972) Fracture of composites. In: Herman H (ed) Treatise on Materials Science and Technology, Vol. 1. Academic, New York, pp 79–114
4. Bader MG, Bailey JE, Curtis PT, Parvizi A (1979) Proceedings of International Conference on Mechanical Behavior of Materials, Cambridge, UK, pp 227–239
5. Bazant ZP, Chen EB (1997) Scaling of structural failure. ASME Appl Mech Rev 50:593
6. Budiansky B (1983) Micromechanics. Comput Struct 16:3–12
7. Cantwell WJ, Morton J (1991) The impact resistance of composite materials – a review. Composites 22:347–362
8. Chan WS (1991) Design approaches for edge delamination resistance in laminated composites. J Compos Tech Res 14:91–96
9. Chung WC, Jang BZ, Chang TC, Hwang LR, Wilcox RC (1989) Fracture behavior in stitched multidirectional composites. Mater Sci Eng A112:157–173
10. Drzal LT (1990) The effect of polymer matrix mechanical properties on the fiber–matrix interfacial strength. Mater Sci Eng A126:2890–2893
11. Elder DJ, Thomson RS, Nguyen MQ, Scott ML (2004) Review of delamination predictive methods for low speed impact of composite laminates. Compos Struct 66:677–683
12. Fabre JP, Sigety P, Jacques D (1991) Stress transfer by shear in carbon fiber model composites. J Mater Sci 26:189–195

13. Flaggs DL, Kural MH (1982) Experimental determination of the in situ transverse lamina strength in graphite/epoxy laminates. J Compos Mater 16:103–116
14. Garrett KW, Bailey JE (1977) Effect of resin failure strain on the tensile properties of glass fiber-reinforced polyester cross-ply laminates. J Mater Sci 12(11):2189–2194
15. Garrett KW, Bailey JE (1977) Multiple transverse fracture in 90 degree cross-ply laminate of a glass-reinforced polyester. J Mater Sci 12(1):157–168
16. Gudmundson P, Östlund S (1992) First order analysis of stiffness reduction due to matrix cracking. J Compos Mater 26:1009–1030
17. Gudmundson P, Zang W (1993) A universal model for thermoelastic properties of macro cracked composite laminates. Int J Solids Struct 30:3211–3231
18. Hahn HT, Tsai SW (1974) On the behavior of composite laminates after initial failures. J Compos Mater 8:288–305
19. Han YM, Hahn HT (1989) Ply cracking and property degradations of symmetric balanced laminates under general in-plane loading. Compos Sci Technol 35:377–397
20. Harris B (1980) Metal Sci 14:351
21. Hashin Z (1985) Analysis of cracked laminates: a variational approach. Mech Mater 4:121–136
22. Hashin Z (1988) Thermal expansion coefficients of cracked laminates. Compos Sci Technol 31:247–260
23. Hashin Z (1990) Analysis of damage in composite materials In: Boehler JP (ed) Yielding, Damage, and Failure of Anisotropic Solids. Mechanical Engineering Publications, London, pp 3–32
24. Henstenburg RB, Phoenix SL (1989) Interfacial shear strength studies using single filament composite test. Polym Compos 10:389–408
25. Highsmith AL, Reifsnider KL (1982) Stiffness-reduction mechanisms in composite laminates, Damage in Composite Materials. ASTM STP 115:103–117
26. Hsueh CH (1992) Interfacial debonding and fiber pull-out stresses of fiber-reinforced composites. Mater Sci Eng A154:125–132
27. Jamison RD, Schulte K, Reifsnider KL, Stinchcomb WW (1984) Characterization and analysis of damage mechanisms in tension–tension fatigue of graphite/epoxy laminates. In: Effects of Defects in Composite Materials, ASTM STP 836, American Society for Testing and Materials, Philadelphia, pp 21–55
28. Jang BZ, Cholakara M, Jang BP, Shih WK (1991) Mechanical properties in multidimensional composites. Polym Eng Sci 31:40–46
29. Jones FR, Wheatley AR, Bailey JE (1981) In: Marshall IH (ed) Composite Structures. Applied Science Publishers, Barking, UK, pp 415–429
30. Kachanov LM (1958) On the creep fracture time (in Russian). Izv AN SSSR, Ofd Tekhn Nauk 8:26–31
31. Kachanov M (1980) Continuum model of medium with cracks. J Eng Mech Div ASCE 106(EM5):1039–1051
32. Kachanov M (1994) Elastic solids with many cracks and related problems. Adv Appl Mech 30:259

33. Kim JK, Mai Y (1991) High strength, high fracture toughness fiber composites with interface control – a review. Compos Sci Technol 41(4):333–378
34. Krajcinovic D (1996) Damage Mechanics. Elsevier, Amsterdam
35. Krajcinovic D (1996) Essential structure of the damage mechanics theories. In: Tatsumi T, Watanabe E, Kambe T (eds) Theoretical and Applied Mechanics. Elsevier, Amsterdam, pp 411–426
36. Lacy TE, McDowell DL, Talreja R (1999) Gradient concepts for evolution of damage. Mech Mater 31:831–861
37. Lafarie-Frenot MC, Hénaff-Gardin C, Gamby D (2001) Matrix cracking induced by cyclic ply stresses in composite laminates. Compos Sci Technol 61(15):2327–2336
38. Lauke BW, Beckert W, Singletary J (1996) Energy release rate and stress field calculation for debonding crack extension at the fiber–matrix interface during single-fiber pull-out. Compos Interface 3:263–273
39. Lim SG, Hong CS (1989) Prediction of transverse cracking and stiffness reduction in cross-ply laminate composites. J Compos Mater 23:695–713
40. Liu D (1990) Delamination resistance in stitched and unstitched composite planes subjected to composite loading. J Reinf Plast Compos 9:59–69
41. Marshall DB, Evans AG (1985) Failure mechanisms in ceramic-fiber/ceramic-matrix composites. J Am Ceram Soc 68:225
42. Mayadas A, Pastore C, Ko FK (1985) Tensile and shear properties of composites by various reinforcement concepts. In: Proceedings of 30th International SAMPE Syrup, pp 1284–1293
43. McCartney LN (1992) Theory of stress transfer in 0–90–0 crossply laminate containing a parallel array of transverse cracks. J Mech Phys Solids 40:27–68
44. Nairn JA (2000) Matrix microcracking in composites. In: Talreja R, Månson JAE (eds) Polymer Matrix Composites, Comprehensive Composite Materials, Vol. 2. Elsevier Science, Amsterdam, pp 403–432
45. Nairn JA, Hu S (1994) Micromechanics of damage: a case study of matrix microcracking. In: Talreja R (ed) Damage Mechanics of Composite Materials, Chapter 6. Elsevier, The Netherlands, pp 117–138
46. Niu K, Talreja R (1999) Modeling of wrinkling in sandwich panels under compression. J Eng Mech 125:875–883
47. Pagano NJ (1998) On the micromechanical failure modes in a class of ideal brittle matrix composites. Part 1. Coated-fiber composites. Compos Part B: Eng 29(2):93–119
48. Parvizi A, Bailey JE (1978) On multiple transverse cracking in glass fiber epoxy cross-ply laminates. J Mater Sci 13(10):2131–2136
49. Parvizi A, Garrett KW, Bailey JE (1978) Constrained cracking in glass fibre-reinforced epoxy cross-ply laminates. J Mater Sci 13:195–201
50. Prichard JC, Hogg PJ (1990) The role of impact damage in post-impacted compression testing. Composites 21:503–511
51. Rosen BW (1964) Tensile failure of fibrous composites. AIAA J 2:1985–1991
52. Smith PA, Boniface L, Glass NFC (1998) Comparison of transverse cracking phenomena in (0/90)s and (90/0)s CFRP laminates. Appl Compos Mater 5:11–23

53. Sørensen BF, Talreja R (1993) Analysis of damage in a ceramic matrix composite. Int J Damage Mech 2:246–271
54. Stinchcomb WW, Reifsnider KL, Yeung P, Masters J (1981) Effect of ply constraint on fatigue damage development in composite material laminates. ASTM STP 723:64–84
55. Su KB (1989) Delamination resistance of stitched thermoplastic matrix composite laminates. ASTM STP 1044:279–300
56. Talreja R (1985) Transverse cracking and stiffness reduction in composite laminates. J Compos Mater 19:355–374
57. Talreja R (1986) Stiffness properties of composite laminates with matrix cracking and internal delaminations. Eng Fract Mech 25:751–762
58. Talreja R (1990) Internal variable damage mechanics of composite materials, Invited Paper. In: Boehler JP (ed) Yielding, Damage and Failure of Anisotropic Solids. Mechanical Engineering Publications, London, pp 509–533
59. Talreja R (1991) Continuum modeling of damage in ceramic matrix composites. Mech Mater 12:165–180
60. Talreja R (1996) A synergistic damage mechanics approach to durability of composite material systems. In: Cardon A, Fukuda H, Reifsnider K (eds) Progress in Durability Analysis of Composite Systems. A.A. Balkema, Rotterdam, pp 117–129
61. Talreja R (2006) Multiscale modeling in damage mechanics of composite materials. J Mater Sci 41(20):6800–6812
62. Tan SC, Nuismer RJ (1989) A theory for progressive matrix cracking in composite laminates. J Compos Mater 23:1029–1047
63. Tong J, Guild FJ, Ogin SL, Smith PA (1997) On matrix crack growth in quasi-isotropic laminates. II. Finite element analysis. Compos Sci Technol 57(11):1537–1545
64. Vakulenko AA, Kachanov ML (1971) Continuum theory of a medium with cracks (in Russian). Izv AN SSSR, Mekh Tverdogo Tela 6:159
65. Varna J, Berglund LA (1991) Multiple transverse cracking and stiffness reduction in cross-ply laminates. J Compos Technol Res 13:97–106
66. Varna J, Krasnikovs A (1998) Transverse cracks in cross-ply laminates. 2. Stiffness degradation. Mech Compos Mater 34(2):153–170
67. Varna J, Akshantala NV, Talreja R (1999) Crack opening displacement and the associated response of laminates with varying constraints. Int J Damage Mech 8:174–193
68. Varna J, Joffe R, Akshantala NV, Talreja R (1999) Damage in composite laminates with off-axis plies. Compos Sci Technol 59:2139–2147
69. Varna J, Joffe R, Talreja R (2001) A synergistic damage mechanics analysis of transverse cracking in $[\pm\theta, 90_4]_s$ laminates. Compos Sci Technol 61:657–665
70. Varna J, Krasnikovs A, Kumar R, Talreja R (2004) A synergistic damage mechanics approach to viscoelastic response of cracked cross-ply laminates. Int J Damage Mech 13(4):301–334

71. Verpoest I, Wevers M, DeMeester P, Declereq P (1989) 2D and 3D fabrics for delamination resistant composite laminates and sandwich structure. SAMPE J 25:51–56
72. Whitney JM, Drzal LT (1987) Axisymmetric stress distribution around an isolated fiber fragment. In: Johnson NJ (ed) Toughened Composites, ASTM STP 937. American Society for Testing and Materials, Philadelphia, pp 176–196
73. Zhou LM, Kim JK, Mai YW (1992) Interfacial debonding and fiber pull-out stresses. J Mater Sci 27:3155–3166